Neurobiology of Aging 65 (2018) 18–40

Contents lists available at ScienceDirect

Neurobiology of Aging

journal homepage: www.elsevier.com/locate/neuaging

Abnormalities of resting-state functional cortical connectivity in patients with dementia due to Alzheimer's and Lewy body diseases: an EEG study

Claudio Babiloni [a,b,*], Claudio Del Percio [c], Roberta Lizio [a,b], Giuseppe Noce [c], Susanna Lopez [a], Andrea Soricelli [c,d], Raffaele Ferri [e], Flavio Nobili [f], Dario Arnaldi [f], Francesco Famà [f], Dag Aarsland [g], Francesco Orzi [h], Carla Buttinelli [h], Franco Giubilei [h], Marco Onofrj [i], Fabrizio Stocchi [b], Paola Stirpe [b], Peter Fuhr [j], Ute Gschwandtner [j], Gerhard Ransmayr [k], Heinrich Garn [l], Lucia Fraioli [m], Michela Pievani [n], Giovanni B. Frisoni [n,o], Fabrizia D'Antonio [p], Carlo De Lena [p], Bahar Güntekin [q], Lutfu Hanoğlu [r], Erol Başar [s], Görsev Yener [s], Derya Durusu Emek-Savaş [t], Antonio Ivano Triggiani [u], Raffaella Franciotti [i], John Paul Taylor [v], Laura Vacca [b,w], Maria Francesca De Pandis [m], Laura Bonanni [i]

[a] Department of Physiology and Pharmacology "Vittorio Erspamer", University of Rome "La Sapienza", Rome, Italy
[b] Institute for Research and Medical Care, IRCCS San Raffaele Pisana, Rome, Italy
[c] Department of Integrated Imaging, IRCCS SDN, Naples, Italy
[d] Department of Motor Sciences and Healthiness, University of Naples Parthenope, Naples, Italy
[e] Department of Neurology, IRCCS Oasi Institute for Research on Mental Retardation and Brain Aging, Troina, Enna, Italy
[f] Clinical Neurology, Department of Neuroscience (DiNOGMI), University of Genoa and IRCCS AOU S Martino-IST, Genoa, Italy
[g] Department of Old Age Psychiatry, King's College University, London, UK
[h] Department of Neuroscience, Mental Health and Sensory Organs, University of Rome "La Sapienza", Rome, Italy
[i] Department of Neuroscience Imaging and Clinical Sciences and CESI, University G d'Annunzio of Chieti-Pescara, Chieti, Italy
[j] Universitätsspital Basel, Abteilung Neurophysiologie, Basel, Switzerland
[k] Department of Neurology and Psychiatry and Faculty of Medicine, Johannes Kepler University Linz, General Hospital of the City of Linz, Linz, Austria
[l] AIT Austrian Institute of Technology GmbH, Vienna, Austria
[m] Hospital San Raffaele of Cassino, Cassino, Italy
[n] Laboratory of Alzheimer's Neuroimaging and Epidemiology, IRCCS Istituto Centro San Giovanni di Dio Fatebenefratelli, Brescia, Italy
[o] Memory Clinic and LANVIE - Laboratory of Neuroimaging of Aging, University Hospitals and University of Geneva, Geneva, Switzerland
[p] Department of Neurology and Psychiatry, Sapienza, University of Rome, Rome, Italy
[q] Department of Biophysics, Istanbul Medipol University, Istanbul, Turkey
[r] Department of Neurology, University of Istanbul-Medipol, Istanbul, Turkey
[s] IBG, Departments of Neurology and Neurosciences, Dokuz Eylül University, Izmir, Turkey
[t] Department of Psychology and Department of Neurosciences, Dokuz Eylül University, Izmir, Turkey
[u] Department of Clinical and Experimental Medicine, University of Foggia, Foggia, Italy
[v] Institute of Neuroscience, Newcastle University, Newcastle, UK
[w] Casa di Cura Privata del Policlinico (CCPP) Milano SpA, Milan, Italy

ARTICLE INFO

Article history:
Received 19 July 2017
Received in revised form 21 December 2017
Accepted 21 December 2017
Available online 30 December 2017

Keywords:
Functional brain connectivity
Resting-state EEG rhythms

ABSTRACT

Previous evidence showed abnormal posterior sources of resting-state delta (<4 Hz) and alpha (8–12 Hz) rhythms in patients with Alzheimer's disease with dementia (ADD), Parkinson's disease with dementia (PDD), and Lewy body dementia (DLB), as cortical neural synchronization markers in quiet wakefulness. Here, we tested the hypothesis of additional abnormalities in functional cortical connectivity computed in those sources, in ADD, considered as a "disconnection cortical syndrome", in comparison with PDD and DLB. Resting-state eyes-closed electroencephalographic (rsEEG) rhythms had been collected in 42 ADD, 42 PDD, 34 DLB, and 40 normal healthy older (Nold) participants. Exact low-resolution brain electromagnetic tomography (eLORETA) freeware estimated the functional lagged linear connectivity

* Corresponding author at: Department of Physiology and Pharmacology, "V. Erspamer" University of Rome, "La Sapienza" P. le A. Moro 5, 00185, Rome, Italy. Tel.: +39 0649910989; fax: +39 0649910917.
E-mail address: claudio.babiloni@uniroma1.it (C. Babiloni).

0197-4580/$ – see front matter
https://doi.org/10.1016/j.neurobiolaging.2017.12.023

Neurodegenerative diseases
Dementia
Alzheimer's disease
Parkinson's disease
Dementia with Lewy bodies

(LLC) from rsEEG cortical sources in delta, theta, alpha, beta, and gamma bands. The area under receiver operating characteristic (AUROC) curve indexed the classification accuracy between Nold and diseased individuals (only values >0.7 were considered). Interhemispheric and intrahemispheric LLCs in widespread delta sources were abnormally higher in the ADD group and, unexpectedly, normal in DLB and PDD groups. Intrahemispheric LLC was reduced in widespread alpha sources dramatically in ADD, markedly in DLB, and moderately in PDD group. Furthermore, the interhemispheric LLC in widespread alpha sources showed lower values in ADD and DLB than PDD groups. At the individual level, AUROC curves of LLC in alpha sources exhibited better classification accuracies for the discrimination of ADD versus Nold individuals (0.84) than for DLB versus Nold participants (0.78) and PDD versus Nold participants (0.75). Functional cortical connectivity markers in delta and alpha sources suggest a more compromised neurophysiological reserve in ADD than DLB, at both group and individual levels.

1. Introduction

Differential diagnosis of Alzheimer's disease dementia (ADD), Parkinson's disease dementia (PDD), and Lewy body dementia (DLB) is important as patients with DLB and PDD may be considerably more sensitive to adverse effects of neuroleptic (Ballard et al., 1998) and may exhibit faster disease progression (Olichney et al., 1998) and different responses to acetylcholinesterase inhibitors (AChEIs) (Levy et al., 1994); furthermore, these diseases have at least in part different etiologies and might require specific disease-modifying regimens when available (Bhat et al., 2015; Karantzoulis and Galvin, 2013; McKeith et al., 2005).

In the light of the new international criteria (Albert et al., 2011; Dubois et al., 2014), AD may be discriminated from PD and DLB by higher abnormalities in the cerebrospinal fluid (CSF) "$A\beta_{42}$/phospho-tau" ratio and deposition of $A\beta_{42}$ or tau in the brain as shown by positron emission tomography (PET) mapping. Other useful topographic biomarkers of AD neurodegeneration are hypometabolism of the posterior cerebral cortex as revealed by ^{18}F-fluorodeoxyglucose PET and hippocampal atrophy on magnetic resonance imaging (MRI), (Albert et al., 2011; Dubois et al., 2014; McKhan et al., 2011). A PET or single-photon emission computed tomography (SPECT) scan of the dopamine transporter can also be used for the differential diagnosis between PDD and DLB on one side and ADD on the other side (Zhu et al., 2014). Promising candidate topographic biomarkers are those derived from the analysis of resting-state eyes-closed electroencephalographic (rsEEG) rhythms (Breslau et al., 1989; Briel et al., 1999; Giaquinto and Nolfe, 1986). The recording of rsEEG rhythms is noninvasive and cost-effective. Markers of rsEEG rhythms may probe the neurophysiological "reserve" in patients with dementing disorders; the latter is defined as the residual ability of the brain to ensure (1) the synchronization of neural activity at different spatial scales and frequencies from small cellular populations to large regions and (2) the coordination of this synchronization across subcortical and cortical neural networks (Babiloni et al., 2016a). The neurophysiological reserve can thus be considered as one of the dimensions of the brain reserve (Stern, 2017). In this line, the assessment of the neurophysiological "reserve" in neurological patients can be based on 2 main classes of markers derived from rsEEG rhythms, namely the cortical neural "synchronization/desynchronization" at given frequency bands and "functional cortical connectivity", defined as the interdependence of cortical neural synchronization/desynchronization intrahemispherically and interhemispherically (Babiloni et al., 2016a). Practically, this connectivity can be computed from rsEEG rhythms recorded at electrode pairs or estimated in coupled cortical sources (Babiloni et al., 2016a).

Functional cortical connectivity might be especially relevant to understand the pathophysiological mechanisms underlying different dementing disorders, as human cognition is based on a coordinated neurotransmission within large-scale networks (D'Amelio and Rossini, 2012; Pievani et al., 2011). Clinically, ADD typically presents with a major amnestic syndrome although there may be, less commonly, linguistic, visuospatial, and visual disease variants (Dubois et al., 2014). PDD and DLB manifest with attentional, verbal, and executive cognitive deficits in association with motor manifestations such as bradykinesia, tremor, postural instability, and rigidity (Aarsland et al., 2003; Buter et al., 2008; Dubois and Pillon, 1997; Emre et al., 2007; Huber et al., 1989; Hughes et al., 2000; Levy et al., 2000; Walker et al., 2015; Wolters, 2001). Motor symptoms substantially precede cognitive deficits in PD but not DLB where the onset of motor symptoms is either at the same time as the cognitive deficits or emerges later. Furthermore, DLB is primarily characterized by visual hallucinations, rapid eye movement (REM) sleep disturbances, and diurnal cognitive fluctuation (McKeith et al., 2005). It can be speculated that those different clinical phenotypes are related to different abnormalities in "synchronization/desynchronization" and "cortical functional connectivity" markers of rsEEG rhythms.

Concerning the "synchronization/desynchronization" markers, previous studies showed that compared with normal healthy older (Nold) participants, ADD patients are characterized by lower power density in posterior alpha (8–12 Hz) and beta (13–30 Hz) rhythms (Babiloni et al., 2006a; Dierks et al., 1993, 2000; Huang et al., 2000; Jelic et al., 2000; Jeong, 2004; Ponomareva et al., 2003). Furthermore, ADD patients exhibit higher power density in widespread delta (<4 Hz) and theta (4–7 Hz) rhythms (Brassen and Adler, 2003; Kogan et al., 2001; Onofrj et al., 2003; Reeves et al., 2002; Rodriguez et al., 2002; Valladares-Neto et al., 1995). Similarly, PDD patients demonstrate widespread high power density in delta and theta rhythms and some reduction of alpha power density (Bonanni et al., 2008; Bosboom et al., 2006, 2009; Caviness et al., 2016; Fünfgeld, 1995; Kamei et al., 2010; Melgari et al., 2014; Neufeld et al., 1988, 1994; Pugnetti et al., 2010; Serizawa et al., 2008; Soikkeli et al., 1991; Stam et al., 2006). DLB patients are characterized by diffuse and fluctuating delta and theta power density with some frequency spectra differences from those observed in PDD and ADD; these EEG features are described as a "supportive" biomarker in the clinical diagnostic guidelines (Andersson et al., 2008; Bonanni et al., 2008, 2015, 2016; Kai et al., 2005; McKeith et al., 2005, 2017; Onofrj et al., 2003; Walker et al., 2000a,b).

As far as the "functional cortical connectivity" markers are concerned, previous studies showed that compared with Nold participants, ADD patients point to lower spectral coherence between electrode pairs in posterior alpha (8–12 Hz) and beta (13–20 Hz) rhythms (Adler et al., 2003; Anghinah et al., 2000; Besthorn et al., 1994; Dunkin et al., 1994; Fonseca et al., 2011, 2013; Jelic et al., 1997, 2000; Knott et al., 2000; Leuchter et al., 1987, 1992; Locatelli et al., 1998; Pogarell et al., 2005; Sloan et al., 1994). However, these effects are topographically variable being observed in temporo-parieto-occipital electrode pairs in some studies (Adler et al., 2003; Locatelli et al., 1998; Jelic et al., 1997, 2000) yet in

other studies in frontocentral electrode pairs (Besthorn et al., 1994; Fonseca et al., 2013; Leucther et al., 1994). Furthermore, some studies report a coherence decrease of rsEEG rhythms at low frequencies, especially at central electrodes in the theta band (Adler et al., 2003; Knott et al., 2000). Other studies report an increase in widespread delta coherences (Babiloni et al., 2010; Locatelli et al., 1998) or a quite complex topographical pattern of coherence increases and decreases (Sankari et al., 2011). Moreover, studies using alternative techniques measuring rsEEG functional coupling show a decrement of synchronization likelihood in frontoparietal alpha rhythms in ADD and mild cognitive impairment (MCI) patients compared with Nold participants (Babiloni et al., 2004, 2006b). Finally, the global beta phase lag index across all scalp electrode pairs was lower in ADD patients compared with Nold participants (Stam et al., 2007).

The above rsEEG results have received some clinical validation. In AD individuals, there are correlations between rsEEG coherences and scores of Mini–Mental State Examination (MMSE), as a measurement of global cognitive status and language, memory, and constructional praxis (Fonseca et al., 2011, 2013). These correlations are negative for delta and theta bands and positive for alpha and beta bands (Fonseca et al., 2011). Furthermore, there is an association between rsEEG coherence and periventricular white matter hyperintensities interpreted as due to impairment of neural transmission (Leuchter et al., 1992, 1994).

In PD individuals, abnormal functional cortical connectivity is consistently revealed by rsEEG coherence between electrode pairs. Compared with Nold participants, PD patients show lower local intrahemispheric parietal alpha coherence (Moazami-Goudarzi et al., 2008). Furthermore, intrahemispheric corticocortical frontoparietal alpha and beta coherences are positively correlated with the severity of PD motor symptoms in the patients (Silberstein et al., 2005). Both L-dopa regimen and electrical stimulation of the subthalamic nucleus reduce those coherences in association with an improvement of motor symptoms (Silberstein et al., 2005). Other evidence reveals a positive correlation between PD duration and beta coherence between rsEEG rhythms recorded in supplementary motor and primary motor areas (Pollok et al., 2013).

Concerning the relationship between functional cortical connectivity and cognition, PD patients with cognitive deficits demonstrate a positive correlation between decreased intrahemispheric frontoparietal alpha coherence and executive dysfunctions (Teramoto et al., 2016). Furthermore, PDD patients exhibit greater interhemispheric frontal alpha-beta and intrahemispheric frontooccipital beta coherences than ADD patients do (Fonseca et al., 2013).

In line with ADD and PDD patients, DLB participants show a derangement of functional cortical connectivity derived from rsEEG rhythms. Global delta and alpha coherences across all electrode pairs are reported as higher in DLB than ADD patients (Andersson et al., 2008). In contrast, the global alpha phase lag index across all electrode pairs is lower in DLB than both ADD and Nold participants (van Dellen et al., 2015). Furthermore, intrahemispheric fronto-temporo-central delta and theta coherences are higher in DLB than ADD patients, whereas temporo-centro-parieto-occipital beta (not alpha) coherences are lower in the former compared with the latter (Kai et al., 2005). Finally, posterior-to-anterior directed information flow is lower in alpha in DLB patients and decreases in beta in ADD patients (Dauwan et al., 2016a).

The above measurements of rsEEG functional connectivity have been successfully used to discriminate ADD, PDD, and DLB individuals. Global delta and alpha coherences between electrode pairs allow for a classification accuracy (area under receiver operating characteristic [AUROC] curve) of DLB individuals compared with ADD and Nold participants of 0.75–0.80 and 0.91–0.97 (e.g., 1 = 100% of accuracy), respectively (Andersson et al., 2008). A complex step-wise procedure using 20-discriminant scalp rsEEG power density and coherences as an input to a statistical pattern recognition method shows a classification accuracy (AUROC curve) of 0.90 between ADD and Nold individuals as well as between ADD and PDD participants (Engedal et al., 2015). Another recent study in relatively small populations of ADD, PDD/DLB, and frontotemporal dementia patients used 25-discriminant scalp rsEEG power density and functional cortical connectivity (i.e., Granger causality) variables as an input to support vector machine, reaching a classification accuracy of 1.0 (Garn et al., 2017). Paradoxically, another study combining quantitative rsEEG variables (including those of functional cortical connectivity) with neuropsychological, clinical, neuroimaging, cerebrospinal fluid, and visual EEG data reached "only" a classification accuracy of 0.87 in the discrimination between ADD, PDD, and DLB individuals (Dauwan et al., 2016b).

The interstudy variability of the mentioned results might be due to (1) the analysis of rsEEG data at scalp electrodes pairs and (2) the use of fixed frequency bands for all participants, regardless the frequency "slowing" of rsEEG rhythms in dementia. To mitigate those potential confounding effects on "synchronization/desynchronization" markers, we have recently combined (1) a source estimation technique called exact low-resolution brain electromagnetic tomography (eLORETA; Pascual-Marqui, 2007a) and (2) an analysis of rsEEG rhythms based on the "individual alpha frequency peak" (IAF; Klimesch, 1996, 1999; Klimesch et al., 1998). With this approach, we tested the hypothesis that eLORETA source activity of scalp rsEEG rhythms might reflect different features of abnormal cortical neural synchronization/desynchronization in ADD, PDD, and DLB patients (Babiloni et al., 2017). To that aim, data sets in 42 PDD, 34 DLB, 42 ADD, and 40 Nold participants were analyzed (demography, education, and the MMSE score did not differ between the patients' groups). Results are summarized in the following (Babiloni et al., 2017). The IAF exhibits a marked frequency slowing in the PDD and DLB groups and a moderate frequency slowing in the ADD group. Compared with Nold participants, the 3 patients' groups show lower posterior alpha source activities. This effect is dramatic in the ADD group, marked in the DLB group, and moderate in the PDD group. The 3 patients' groups also exhibit higher occipital delta source activities. This effect is greatest in the PDD group, marked in the DLB group, and moderate in the ADD group.

Concerning the individual level, the posterior delta and alpha sources permitted good classification accuracies (AUROC curve) ranging 0.85–0.90 between the Nold participants and patients as well as between ADD and PDD patients (Babiloni et al., 2017). Those findings unveiled different spatial and frequency features of the cortical neural synchronization/desynchronization underpinning brain arousal in quiet wakefulness in ADD, PDD, and DLB patients where the DLB group showed features in between the ADD and PDD groups.

Keeping in mind those findings and considerations, the present retrospective exploratory study reanalyzed the original rsEEG database used in the study by Babiloni et al. (2017) to derive complementary "functional cortical connectivity" markers. We compared the intrahemispheric and interhemispheric lagged linear connectivity between cortical sources of rsEEG rhythms in Nold, ADD, PDD, and DLB participants. The comparison was made both at the group and the individual level. The core hypothesis was that at both levels, "functional cortical connectivity" markers were globally more altered in ADD patients whose disease has been considered as a cortical "disconnection syndrome" (Besthorn et al., 1994; Bokde et al., 2009; Dunkin et al., 1995; Leuchter et al., 1994; Reuter-Lorenz and Mikels, 2005; Teipel et al., 2016).

2. Materials and methods

Details on the participants, diagnostic criteria, rsEEG recording, and preliminary data analysis were reported in the reference study (Babiloni et al., 2017). In the following sections, we provide a short description of those methodological procedures for readers' convenience.

2.1. Participants and diagnostic criteria

We used the rsEEG data of an international archive, formed by clinical, neuropsychological, and electrophysiological data in 40 Nold, 42 ADD, 42 PDD, and 34 DLB participants. The 4 groups (i.e., PDD, ADD, DLB, and Nold) were carefully matched for age, gender, and education. The 3 groups of patients with dementia were also carefully matched for the MMSE score (Folstein et al., 1975). Table 1 reports details of the aforementioned variables.

Probable ADD was diagnosed according to the criteria of the Diagnostic and Statistical Manual of Mental Disorders, fourth edition, (2000) (DSM-IV-TR; American Psychiatric Association) and the National Institute of Neurological Disorders and Stroke–Alzheimer Disease and Related Disorders Association (NINCDS-ADRDA) working group (McKhann et al., 1984).

The ADD patients underwent general medical, neurological, and psychiatric assessments. They were also rated on some standardized clinical scales that included MMSE (Folstein et al., 1975), clinical deterioration rate (Hughes et al., 1982), 15-item Geriatric Depression Scale (Yesavage et al., 1983), Hachinski Ischemic Score (Rosen et al., 1980), and Instrumental Activities of Daily Living Scale (Lawton and Brodie, 1969). Neuroimaging diagnostic procedures (MRI) and laboratory analyses were carried out to exclude other causes of progressive or reversible dementias, to form a relatively homogenous ADD patient group. Computed tomography was performed in those patients with contraindications to MRI.

Inclusion criteria were as follows: (1) objective impairment on neuropsychological evaluation, as defined by performances under a value of 1.5 standard deviations from the mean value for the age- and education-matched controls in at least 2 cognitive domains; (2) clinical dementia rating score higher than 0.5; and (3) abnormal activities of daily living as attested by the history and evidence of independent living.

Exclusion criteria included any evidence of (1) frontotemporal dementia, diagnosed according to criteria of Lund and Manchester Groups (1994); (2) vascular dementia, diagnosed according to NINDS-AIREN criteria (Roman et al., 1993); (3) extrapyramidal syndromes; (4) reversible dementias (including pseudodementia of depression); and (5) Lewy body disease–associated dementia. A battery of neuropsychological tests assessed general cognitive performance in the domains of memory, language, executive function/attention, and visuoconstruction abilities (for details see Babiloni et al., 2017). Concerning psychoactive medications, most of the enrolled ADD patients (89%) followed a long-term treatment with standard daily doses of AChEIs (e.g., donepezil 5–10 mg/day or rivastigmine 3 mg/day or galantamine 16–36 mg/day). About 2% received N-methyl-D-aspartate receptor (NMDAR) antagonists (e.g., memantine). About 24% nonregularly took antidepressants or sedatives (e.g., fluoxetine, benzodiazepines) drugs.

The diagnosis of PD was based on a standard clinical assessment of tremor, rigidity, and bradykinesia (Gelb et al., 1999). As measures of severity of motor disability, the Hoehn and Yahr stage (Hoehn and Yahr, 1967) and the Unified Parkinson Disease Rating Scale-III (Fahn and Elton, 1987) for extrapyramidal symptoms were used. A diagnosis of PDD was given to the patients with a history of dementia (inclusion criteria as for ADD) preceded by a diagnosis of PD for at least 12 months.

On the basis of clinical features and neuroradiological findings, exclusion criteria for PDD included the following forms of parkinsonism: (1) DLB (McKeith et al., 1996); (2) secondary parkinsonism, including drug-induced parkinsonism; (3) cerebrovascular parkinsonism; and (4) atypical parkinsonism with absent or minimal responses to antiparkinsonian drugs.

All PDD patients underwent a battery of clinical scales including the Neuropsychiatric Inventory (Cummings et al., 1994), the scale for the assessment of Behavioral and Psychological Symptoms of Dementia, the MMSE, the Dementia Rating Scale-2 (Jurica et al., 2001), the Epworth Sleepiness Scale to estimate subjective sleep disturbances, and the Alzheimer's Disease Cooperative Study for the Activities of Daily Living. All PDD participants also underwent a battery of neuropsychological tests (for details see Babiloni et al., 2017). Concerning psychoactive medications, most of the enrolled PDD patients (79%) followed a treatment with standard doses of dopamine agonists (levodopa, carbidopa, entacapone, pramipexole, apomorphine, tolcapone, rasagiline, or rotigotine). About 45% assumed AChEIs (rivastigmine, donepezil, or galantamine), and about 5% received NMDAR antagonists (memantine). Furthermore, about 42% regularly took antidepressants (selective serotonin reuptake inhibitors: sertraline, citalopram, or paroxetine; monoamine oxidase inhibitor: selegiline; noradrenergic and specific serotonergic antidepressant: mirtazapine; serotonin antagonist and reuptake inhibitor: trazodone; or serotonin-norepinephrine reuptake inhibitor: venlafaxine). Finally, about 8% of them took benzodiazepine sedatives (lorazepam or clonazepam), and 37% of them took antipsychotics (quetiapine, clozapine, or aripiprazole).

Dementia was diagnosed in the DLB patients as for the ADD and PDD patients (see above inclusion and exclusion criteria). The diagnosis of probable DLB was carried out in agreement with the consensus guidelines by McKeith et al. (2005). Concerning the detection of the core and suggestive features of DLB, the Neuropsychiatric Inventory item-2 investigated the occurrence frequency and the severity of hallucinations (Cummings et al., 1994). Frontal Assessment Battery (Dubois et al., 2000) and Clinician Assessment of Fluctuations (Walker et al., 2000a) were included to investigate,

Table 1
Mean values (±SE) of the demographic and clinical data as well as the results of their statistical comparisons ($p < 0.05$) in the groups of Nold participants and ADD, PDD, and DLB patients

Mean values (±SE) of demographic data and global cognitive status (MMSE score)					
	Nold	ADD	PDD	DLB	Statistical analysis
N	40	42	42	34	
Age, years	72.9 (±1.1 SE)	73.3 (±1.0 SE)	74.1 (±1.1 SE)	75.1 (±1.1 SE)	ANOVA: n.s.
Gender (M/F)	16/24	17/25	18/24	11/23	Fisher-Freeman-Halton: n.s.
Education	8.5 (±0.6 SE)	8.1 (±0.8 SE)	7.0 (±0.6 SE)	7.4 (±0.8 SE)	ANOVA: n.s.
MMSE	28.7 (±0.2 SE)	18.9 (±0.6 SE)	18.8 (±0.7 SE)	18.6 (±0.8 SE)	Kruskal-Wallis: H=88.7, $p<0.00001$ (Nold > ADD, PDD, and DLB)

Key: ADD, Alzheimer's disease with dementia; ANOVA, analysis of variance; DLB, Lewy body dementia; MMSE, Mini–Mental State Examination; M/F, males/females; n.s., not significant ($p > 0.05$); Nold, normal healthy older; PDD, Parkinson's disease with dementia; SE, standard error of the mean.

respectively, the severity of frontal dysfunctions and the presence and severity of cognitive fluctuations. The Unified Parkinson Disease Rating Scale-III (Fahn and Elton, 1987) assessed the presence and severity of extrapyramidal signs. The presence or absence of REM sleep behavior disorder was determined according to minimal International Classification of Sleep Disorders criteria (2014). All DLB participants also underwent a battery of neuropsychological tests (for details see Babiloni et al., 2017). Concerning psychoactive medications, half of the enrolled DLB patients (50%) followed a treatment with standard doses of dopamine agonists (levodopa, carbidopa, or entacapone). About 25% assumed AChEIs (rivastigmine), and about 13% received NMDAR antagonists (memantine). Furthermore, about 38% regularly took antidepressants (selective serotonin reuptake inhibitor: citalopram or paroxetine). Finally, about 13% of them took benzodiazepine sedatives (lorazepam), and most of them (63%) took antipsychotics (quetiapine or clozapine).

In all ADD, PDD, and DLB patients, drugs were suspended for about 24 hours before EEG recordings. This did not ensure a complete washout of the drug—longer periods would not have been applicable for obvious ethical reasons—but made it comparable to the drug condition in the ADD, PDD, and DLB patients.

All Nold participants underwent a cognitive screening (including MMSE and Geriatric Depression Scale) as well as physical and neurological examinations to exclude any dementia or major cognitive deficit or psychiatric disorder.

2.2. Resting-state eyes-closed EEG recordings and preliminary data analysis

The rsEEG data were recorded in the morning while participants kept their eyes closed in a relaxed state, not moving or talking. About 5 minutes of rsEEG data were recorded (128 Hz or higher sampling rate, with related antialiasing bandpass between 0.01 Hz and 100 Hz) from 19 scalp electrodes positioned according to the 10–20 system (i.e., Fp1, Fp2, F7, F3, Fz, F4, F8, T3, C3, Cz, C4, T4, T5, P3, Pz, P4, T6, O1, and O2). A ground electrode was located in the frontal region. Electrode impedances were kept below 5 kΩ. Horizontal and vertical electrooculographic activities (0.3–70 Hz bandpass) were also recorded to monitor blinking and eye movements. Table 1 in the Supplementary Material reports details about sampling rates, time constants, and digital EEG systems used in all recording units of the present international consortium. Fig. 1 shows representative EEG waveforms (10 seconds) on Fz and Pz scalp electrodes for Nold, ADD, PDD, and DLB participants. These participants were carefully selected to represent the general features of EEG waveforms in the groups of individuals investigated in the present study.

The rsEEG data were divided into segments of 2 seconds and analyzed offline. The epochs affected by any physiological (ocular/blinking, muscular, and head movements) or nonphysiological (bad contact electrode scalp) artifacts were preliminarily identified by an automatic computerized procedure (Moretti et al., 2003). Furthermore, 2 independent experimenters manually checked and (dis) confirmed the artifact-free rsEEG epochs, before successive analyses. Specifically, they controlled for the presence of ocular and blinking artifacts based on electrooculographic signals, whereas muscular and head artifacts were recognized by analyzing EEG signals. Moreover, head artifacts were detected by a sudden and great increase in amplitude of slow EEG waves in all scalp electrodes. Finally, muscle artifacts were recognized by observing the effects of several frequency bandpass filters in different ranges and by the inspection of EEG power density spectra. Muscle tension is related to unusually high and stable values of EEG power density from 30 to 100–150 Hz, which contrast with the typical declining trend of EEG power density from 25 Hz onward. As a result, the 2 experimenters selected 118 (±5 standard error of the mean [SE]) artifact-free EEG epochs in the Nold group, 106 (±7 SE) in the ADD group, 84 (±5 SE) in the PDD group, and 105 (±5 SE) in the DLB group. The artifact-free epochs showed the same proportion of the total amount of rsEEG recorded in all groups (>80%).

A standard digital spectrum analysis, based on fast fourier transform (Welch technique, Hanning windowing function, or no phase shift) computed the power density of scalp rsEEG rhythms with 0.5 Hz of frequency resolution. The frequency bands of interest were individually identified based on the following frequency landmarks: the transition frequency (TF) and the IAF. In the EEG power density spectrum, the TF marked the transition frequency between the theta and alpha bands, defined as the minimum of the rsEEG power density between 3 and 8 Hz (between the delta and the alpha power peak). Instead, the IAF was defined as the maximum power density peak between 6 and 14 Hz. These

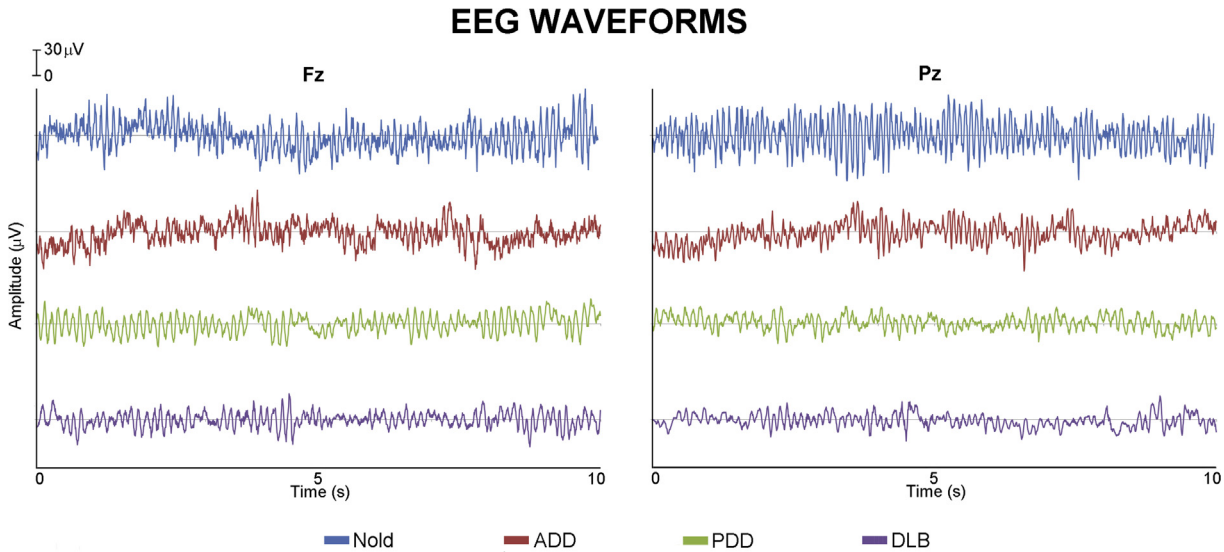

Fig. 1. Representative EEG waveforms (10 seconds) on Fz and Pz scalp electrodes for Nold, ADD, PDD, and DLB participants. These participants were carefully selected to represent the general features of EEG waveforms in the groups of individuals investigated in the present study. Abbreviations: ADD, Alzheimer's disease with dementia; DLB, Lewy body dementia; Nold, normal healthy older; PDD, Parkinson's disease with dementia.

frequency landmarks were originally introduced in the individual frequency analysis of EEG activity by Dr Wolfgang Klimesch (Klimesch, 1996, 1999 and Klimesch et al., 1998). Of note, the relative individual frequency bands are useful to account for the "slowing" in frequency of rsEEG rhythms due to dementing disorders. However, they do not provide a clear cut threshold to discriminate a patient with a dementing disorder from an Nold individual with an innate slowing of that frequency in rsEEG rhythms.

The TF and IAF were computed for each participant involved in the study. Based on the TF and IAF, we estimated the individual delta, theta, and alpha bands as follows: delta from TF − 4 Hz to TF − 2 Hz, theta from TF − 2 Hz to TF, low-frequency alpha (alpha 1 and alpha 2) from TF to IAF, and high-frequency alpha (or alpha 3) from IAF to IAF + 2 Hz. Specifically, the individual alpha 1 and alpha 2 bands were computed as follows: alpha 1 from TF to the frequency midpoint of the TF–IAF range and alpha 2 from that midpoint to IAF. The other bands were defined based on the standard fixed frequency ranges used in the reference study (Babiloni et al., 2017): beta 1 from 14 to 20 Hz, beta 2 from 20 to 30 Hz, and gamma from 30 to 40 Hz.

2.3. Estimation of functional connectivity of rsEEG cortical sources

The eLORETA freeware was used to estimate the functional cortical connectivity from rsEEG rhythms (Pascual-Marqui, 2007a). Specifically, we used the toolbox called lagged linear connectivity (LLC; Pascual-Marqui et al., 2011). LLC provides linear measurements (from now on "LLC solutions") of the statistical interdependence of pairs of eLORETA cortical source activations estimated from scalp rsEEG rhythms at a given frequency. The procedure provides LLC solutions between all combinations of voxels in the cortical source space of eLORETA (Pascual-Marqui et al., 2011). In its practical use, researchers can average those LLC solutions across eLORETA voxels for pairs of regions of interest (ROIs).

Noteworthy, LLC solutions are estimated by removing the zero-lag instantaneous phase interactions between rsEEG cortical sources estimated by eLORETA freeware. The rationale is that these zero-lag phase interactions could be affected by instantaneous physical propagation of neural ionic currents from a given source to all the others merely due to head volume conductor effects (Pascual-Marqui, 2007b). Furthermore, the LLC solutions took into account measures of interdependence among multivariate rsEEG time series, thus partially mitigating the head volume conduction component of the so-called "common drive/source" effect of a "third" source on the LLC solutions estimated between 2 sources of interest (Pascual-Marqui, 2007c). However, the LLC solutions are intrinsically "bivariate" measurements that may not take into account for the "common drive/source" due to the propagation of action potentials along nerves to 2 (or more) target cortical neural populations generating EEG signals. In the case of a "common drive/source", the EEG signals generated from these target populations are expected to be the delayed one in respect to another because of different axon path lengths. As a result, there may be phase differences between them accompanied with high-coherence values not related to a "true" functional connection.

For each participant and frequency band of interest (i.e., delta, theta, alpha 1, alpha 2, alpha 3, beta 1, beta 2, and gamma), LLC solutions were computed for 5 ROIs, namely frontal, central, parietal, occipital, and temporal lobes in the eLORETA cortical source space (Pascual-Marqui, 2007a).

For the interhemispheric analysis, the LLC solutions were calculated between all voxels of the mentioned ROIs of each hemisphere with the homologous ones of the other hemisphere. The LLC solutions for all voxels of a given pair of ROIs were averaged. For each frequency band of interest, the following 5 interhemispheric LLC solutions were computed: frontal (i.e., frontal left–frontal right LLC), central (i.e., central left–central right LLC), parietal (i.e., parietal left–parietal right LLC), occipital (i.e., occipital left–occipital right LLC), and temporal (i.e., temporal left–temporal right LLC).

For the intrahemispheric analysis, the LLC solutions were computed for all voxels of a particular ROI with all voxels of another ROI of the same hemisphere. The LLC solutions for all voxels of a given pair of ROIs were averaged. This operation was repeated for the left hemisphere and the right hemisphere, separately. In particular, for each frequency band of interest and the left hemisphere, the following 5 left intrahemispheric LLC solutions were computed: (1) frontal (i.e., mean among left frontal–central, left frontal–parietal, left frontal–temporal, and left frontal–occipital LLC); (2) central (i.e., mean among left central–frontal, left central–parietal, left central–temporal, and left central–occipital LLC); (3) parietal (i.e., mean among left parietal–frontal, left parietal–central, left parietal–temporal, and left parietal–occipital LLC); (4) occipital (i.e., mean among left occipital–frontal, left occipital–central, left occipital–parietal, and left occipital–temporal LLC); and 5) temporal (i.e., mean among left temporal–frontal, left temporal–central, left temporal–parietal, and left temporal–occipital LLC). The same procedure was repeated for the right hemisphere.

Table 2 reports the Talairach coordinates of the centroid voxel for the left and right frontal, central, parietal, occipital, and temporal ROIs.

2.4. Statistical analysis of the LLC of rsEEG cortical sources

The main statistical session was performed by the commercial tool STATISTICA 10 (StatSoft Inc, www.statsoft.com) to test the hypothesis that the functional cortical connectivity as revealed by the eLORETA LLC solutions between rsEEG source pairs (hereinafter LLC solutions) might differ between the ADD, PDD, and DLB groups, using the Nold group as a control reference. To this aim, 2 analyses of variance (ANOVAs) were computed using the eLORETA LLC solutions as dependent variables ($p < 0.05$).

The first ANOVA tested the differences of interhemispheric LLC solutions between the ADD, PDD, and DLB groups using the Nold group as a control reference. The ANOVA factors were Group (Nold, ADD, PDD, and DLB), Band (delta, theta, alpha 1, alpha 2, alpha 3, beta 1, beta 2, and gamma), and ROI (frontal, central, parietal, occipital, and temporal).

The second ANOVA tested the differences of intrahemispheric LLC solutions between the ADD, PDD, and DLB groups using the Nold group as a control reference. The ANOVA factors were Group (Nold, ADD, PDD, and DLB), Hemisphere (left and right), Band (delta, theta, alpha 1, alpha 2, alpha 3, beta 1, beta 2, and gamma), and ROI (frontal, central, parietal, occipital, temporal, and limbic).

Table 2
Talairach coordinates of the centroid voxel for the left and right frontal, central, parietal, occipital, and temporal regions of interest

Regions of interest	X	Y	Z
Left frontal	−27.9	35.2	10.6
Left central	−32.6	−12.7	52.3
Left parietal	−33.2	−53.4	39.9
Left occipital	−22.2	−81.0	5.2
Left temporal	−49.6	−22.9	−13.9
Right frontal	27.8	35.4	12.3
Right central	32.5	−12.4	52.5
Right parietal	30.2	−53.5	40.9
Right occipital	20.4	−81.5	5.1
Right temporal	50.2	−21.1	−14.2

Individual TF and the IAF values were used as covariates. Mauchly's test evaluated the sphericity assumption. The degrees of freedom were corrected by the Greenhouse-Geisser procedure when appropriate ($p < 0.05$).

Duncan test was used for post hoc comparisons ($p < 0.05$). The planned post hoc testing evaluated the primary hypothesis about the differences in the LLC solutions between the ADD, PDD, and DLB groups, using the Nold group as a control reference. Specifically, we tested the following predictions: (1) a statistically significant interaction effect including the factor Group ($p < 0.05$) and (2) a post hoc test indicating statistically significant differences in the LLC solutions between the ADD, PDD, DLB, and Nold groups (Duncan test, $p < 0.05$). The input data for the mentioned statistical analyses were controlled by Grubbs' test ($p < 0.0001$) for the presence of outliers in the distribution of the LLC solutions.

As an exploratory statistical analysis at the individual level, the Spearman test evaluated the correlation between the MMSE score and LLC solutions showing statistically significant differences between the Nold and the patients' groups ($p < 0.05$). The correlation analysis was performed considering all Nold, ADD, PDD, and DLB individuals as a whole group for 2 reasons. On the one hand, the hypothesis was that LLC solutions from rsEEG cortical sources were correlated with the global cognitive status in seniors in general, namely including cases with both normal and impaired cognitive functions. On the other hand, the correlation study would have had a low statistical sensitivity if performed only in the separate groups, owing to the very limited scatter of the MMSE scores within a given group (e.g., in Nold participants, MMSE score can just assume discrete values of 30, 29, and 28). To take into account the inflating effects of repetitive univariate tests, the statistical threshold was determined based on the Bonferroni correction at $p < 0.05$.

2.5. Accuracy of the discrimination between the Nold, ADD, PDD, and DLB individuals based on eLORETA LLC solutions

eLORETA LLC solutions showing statistically significant differences ($p < 0.05$) among the 4 groups in the aforementioned ANOVAs (i.e., effects of the factor Group and Duncan post hoc) were used as discriminant variables for the classification of the Nold participants and the demented patients of each pathological group (i.e., Nold vs. ADD, Nold vs. DLB, and Nold vs. PDD) and between the patients of pairs of the pathological groups (i.e., ADD vs. DLB, ADD vs. PDD, and DLB vs. PDD). These classifications were performed by GraphPad Prism software (GraphPad Software, Inc, California, USA) using its implementation of ROC curves (DeLong et al., 1988). The following indexes measured the results of the binary classifications—(1) Sensitivity: It measures the rate of the cases (i.e., patients with dementia in the classifications of those patients and Nold participants) who were correctly classified as cases (i.e., "true positive rate" in the signal detection theory); (2) Specificity: It measures the rate of the controls (i.e., Nold participants in the classifications of those participants and patients with dementia) who were correctly classified as controls (i.e., "true negative rate" in the signal detection theory); (3) Accuracy: It is the mean between the sensitivity and specificity weighted for the number of cases and controls; and (4) AUROC curve: For the sake of brevity, the AUROC curve was used as a major reference index of the global classification accuracy.

3. Results

3.1. Comparison of TF and IAF

Table 3 reports the mean values of TF and IAF for the 4 groups (i.e., Nold, ADD, PDD, and DLB), together with the results of the statistical comparisons between the groups (ANOVA). The mean TF was 5.9 Hz (±0.2 SE) in the Nold, 5.4 Hz (±0.2 SE) in the ADD, 4.8 Hz (±0.1 SE) in the PDD, and 4.9 Hz (±0.1 SE) in the DLB group. The mean IAF was 9.0 Hz (±0.2 SE) in the Nold, 8.0 Hz (±0.3 SE) in the ADD, 7.3 Hz (±0.2 SE) in the PDD, and 7.2 Hz (±0.2 SE) in the DLB group.

The statistical analysis of those values showed the following results. There was a main effect of the ANOVA using the TF as a dependent variable and the factor Group ($F = 10.4$, $p < 0.0001$). Duncan post hoc test showed that the mean TF was greater in the Nold than the ADD ($p < 0.05$), the PDD ($p < 0.00001$), and the DLB group ($p < 0.00005$). Furthermore, the mean TF was higher in the ADD than the PDD ($p < 0.05$) and the DLB group ($p < 0.05$).

Another result was the main effect of the ANOVA using the IAF as a dependent variable and the factor Group ($F = 14.9$, $p < 0.00001$). Duncan post hoc test showed that the mean IAF was greater in the Nold than the ADD ($p < 0.001$), the PDD ($p < 0.00001$), and the DLB group ($p < 0.000005$). The mean IAF was also higher in the ADD than the PDD ($p < 0.05$) and the DLB group ($p < 0.01$).

As a remark, 9 ADD, 2 PDD, and 5 DLB patients exhibited asymptotic rsEEG power spectra, without any alpha power peak. Therefore, they were not considered for the statistical analysis of IAF. For the analysis of LLC solutions, the frequency bands from delta to alpha were determined based on the group mean values of IAF.

3.2. Comparison of eLORETA interhemispheric LLC solutions

Fig. 2 shows mean values (±SE) of the interhemispheric LLC solutions relative to a statistically significant ANOVA interaction effect ($F = 3.3$, $p < 0.0001$) among the factors Group (Nold, ADD, PDD, and DLB), Band (delta, theta, alpha 1, alpha 2, alpha 3, beta 1, beta 2, and gamma), and ROI (frontal, central, parietal, occipital, and temporal). Here, the LLC solutions reflect the statistical interdependence of pairs of homologous eLORETA cortical sources between the 2 hemispheres, estimated from scalp rsEEG rhythms at the frequency bands of interest. In Fig. 2, the profile and magnitude of the interhemispheric LLC solutions clearly differed across the ROIs and frequency bands within and between the Nold, ADD, PDD, and DLB groups, exploiting spatial and frequency information contents of the methodological approach.

In the Nold group, as a physiological reference, dominant values of interhemispheric LLC solutions were observed in temporal (maximum), occipital, and parietal alpha 2 and alpha 3 sources. Low values of interhemispheric LLC solutions were found in the widespread delta, theta, and alpha 1 sources. The LLC solutions in beta 1, beta 2, and gamma sources were close to zero, possibly confirming the lack of ocular, head, and muscular artifacts in the EEG data. Summarizing, the Nold group was characterized by a prominent interhemispheric functional connectivity between posterior cortical sources from moderate- to high-frequency alpha rhythms.

Compared with the Nold group, the 3 patients' groups (i.e., ADD, PDD, and DLB) showed a similar spatial and frequency profile of interhemispheric LLC solutions but a lower magnitude in the alpha range (beta 1, beta 2, and gamma sources were close to zero as in the Nold group). Specifically, there was a substantial decrease of the interhemispheric LLC solutions in parietal, occipital, and temporal alpha 2 and alpha 3 sources, which was maximum in the ADD group. Furthermore, interhemispheric LLC solutions in delta sources generally showed a diffuse and very slight increase in the patients' groups. The only exception was a more consistent increase of LLC solutions in delta sources in the ADD group.

Duncan planned post hoc testing revealed that the discriminant LLC pattern ADD < DLB < PDD < Nold was fitted only by the occipital and temporal alpha 3 sources ($p < 0.05$ to 0.000001), which

Table 3
Mean values (±SE) of TF and IAF of the rsEEG power density spectra in the Nold, ADD, PDD, and DLB groups

Mean values (±SE) of theta/alpha TF and IAF					
	Nold	ADD	PDD	DLB	Statistical analysis
TF	5.8 (±0.2 SE)	5.9 (±0.2 SE)	4.9 (±0.2 SE)	5.0 (±0.2 SE)	ANOVA: F = 10.4, $p < 0.00001$ (Nold > ADD > PDD and DLB)
IAF	9.0 (±0.2 SE)	8.8 (±0.3 SE)	7.3 (±0.3 SE)	7.3 (±0.3 SE)	ANOVA: F = 14.9, $p < 0.00001$ (Nold > ADD > PDD and DLB)

The table also reports the p values derived from the statistical comparisons of these values between the groups. See Methods for the definition of the TF and IAF.
Key: ADD, Alzheimer's disease with dementia; ANOVA, analysis of variance; DLB, dementia with Lewy body; IAF, individual alpha frequency peak; Nold, normal healthy older; PDD, Parkinson's disease with dementia; rsEEG, resting-state eyes-closed electroencephalographic; SE, standard error of the mean; TF, transition frequency.

decreased dramatically in the ADD group ($p < 0.000001$), markedly in the DLB group ($p < 0.000001$), and moderately in the PDD group ($p < 0.005$) compared with the Nold group. This interhemispheric effect was most effective in differentiating the 3 neurodegenerative dementing disorders at the group level.

Duncan planned post hoc testing revealed that the discriminant LLC pattern ADD < DLB < PDD < Nold was fitted only by the occipital and temporal alpha 3 sources ($p < 0.05$ to 0.000001), which decreased dramatically in the ADD group ($p < 0.000001$), markedly in the DLB group ($p < 0.000005$), and moderately in the PDD group ($p < 0.01$) compared with the Nold group. This interhemispheric effect was most effective in differentiating the 3 neurodegenerative dementing disorders at the group level.

Another finding was the discriminant LLC pattern ADD < DLB and PDD < Nold, fitted only by the occipital and temporal alpha 2 sources ($p < 0.005$ to 0.000001). Those discriminant LLC solutions pointed to a dramatic reduction in the ADD group ($p < 0.000001$) and a marked reduction in both DLB and PDD groups ($p < 0.005$) when compared with the Nold group. This interhemispheric effect was most effective in differentiating ADD versus DLB/PDD at the group level.

The discriminant LLC pattern ADD and DLB < PDD < Nold was fitted only by the parietal alpha 2 and alpha 3 sources ($p < 0.005$ to 0.000005). Those discriminant LLC solutions indicated a dramatic reduction in the ADD and DLB groups ($p < 0.000005$) and a marked reduction in the PDD group ($p < 0.0001$) in relation to the Nold group. This interhemispheric effect was most effective in differentiating ADD/DLB versus PDD at the group level.

Finally, interhemispheric LLC solutions in delta sources showed only a unique effect in the occipital delta sources, namely greater solutions in the ADD than the Nold and PDD groups ($p < 0.05$).

3.3. Comparison of eLORETA intrahemispheric LLC solutions

Fig. 3 plots mean values (±SE) of the intrahemispheric LLC solutions relative to a statistically significant ANOVA interaction effect (F = 3.2, $p < 0.0001$) among the factors Group (Nold, ADD, PDD, and DLB), Band (delta, theta, alpha 1, alpha 2, alpha 3, beta 1, beta 2, and

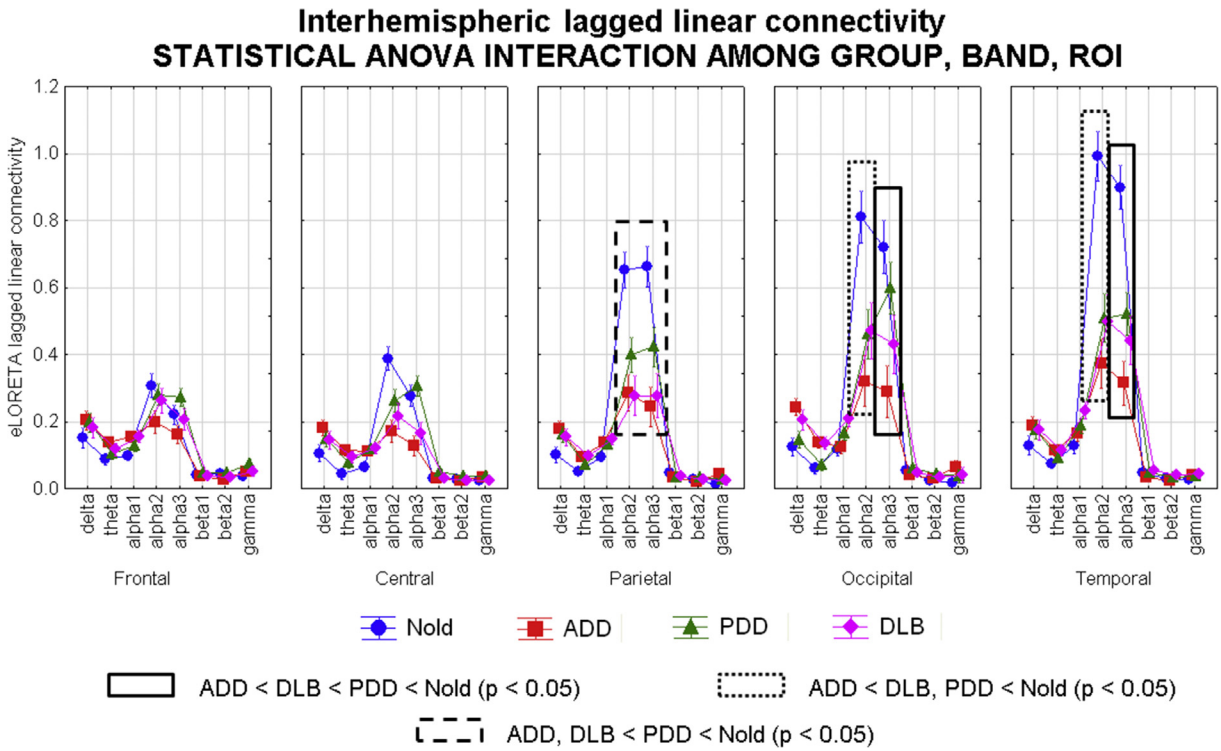

Fig. 2. Mean values (±SE) of the interhemispheric LLC solutions computed in eLORETA cortical sources of resting-state electroencephalographic rhythms (rsEEG) relative to a statistically significant ANOVA interaction effect (F = 3.2, $p < 0.0001$) among the factors Group (Nold, ADD, PDD, and DLB), Band (delta, theta, alpha 1, alpha 2, alpha 3, beta 1, beta 2, and gamma), and ROI (frontal, central, parietal, occipital, and temporal). The rectangles indicate the ROIs and frequency bands in which the interhemispheric LLC solutions presented statistically significant differences among the four groups of participants ($p < 0.05$). Abbreviations: ADD, Alzheimer's disease with dementia; ANOVA, analysis of variance; DLB, Lewy body dementia; eLORETA, exact low-resolution brain electromagnetic tomography; LLC, lagged linear connectivity; Nold, normal healthy older; PDD, Parkinson's disease with dementia; ROI, region of interest; rsEEG, resting-state eyes-closed electroencephalographic; SE, standard error of the mean.

gamma), and ROI (frontal, central, parietal, occipital, and temporal). Noteworthy, there was no effect of the factor Hemisphere (left and right), pointing to a substantial symmetry of the intrahemispheric LLC solutions on the left and the right side. In Fig. 3, the profile and magnitude of the intrahemispheric LLC solutions clearly differed across the ROIs and frequency bands within and between the Nold, ADD, PDD, and DLB groups.

In the Nold group as a reference, dominant values of intrahemispheric LLC solutions were observed in temporal (maximum), occipital, and parietal alpha 2 and alpha 3 sources, whereas moderate values were found in central and frontal alpha 2 and alpha 3 sources. Low interhemispheric LLC solutions were found in the delta, theta, and alpha 1 sources in all ROIs. As for the interhemispheric LLC solutions, the intrahemispheric LLC solutions in beta 1, beta 2, and gamma sources were close to zero, possibly confirming the lack of ocular, head, and muscular artifacts in the EEG data. On the whole, the Nold group was characterized by a prominent intrahemispheric functional connectivity in widespread cortical sources of moderate- to high-frequency alpha rhythms.

As for the intrahemispheric LLC solutions, the 3 patients' groups (i.e., ADD, PDD, and DLB) showed a similar spatial and frequency profile of intrahemispheric LLC solutions but a lower magnitude in the alpha range (beta 1, beta 2, and gamma sources were close to zero as in the Nold group). Specifically, there was a substantial decrease of the intrahemispheric LLC solutions in central, parietal, occipital, and temporal alpha 2 and alpha 3 sources, which was maximum in the ADD and DLB groups. Furthermore, intrahemispheric LLC solutions in delta sources generally showed a diffuse but slight increase in the patients' groups. The only exception was a more consistent increase in those solutions in temporal, parietal, and occipital delta sources in the ADD group.

In contrast to the interhemispheric LLC solutions, Duncan planned post hoc testing revealed no significant discriminant LLC pattern ADD < DLB < PDD < Nold ($p > 0.05$) for the intrahemispheric LLC solutions, mostly due to the similar profiles of the latter in the ADD and DLB groups.

An interesting finding was the discriminant LLC pattern ADD and DLB < PDD < Nold fitted by many sources, namely the central, parietal, temporal, and occipital alpha 2 and alpha 3 sources ($p <$ 0.0005 to <0.000001). These discriminant intrahemispheric LLC solutions showed a dramatic reduction in the ADD and DLB groups ($p < 0.000001$), whereas the decrease was moderate in the PDD group ($p < 0.00005$) as compared with the Nold group. This intrahemispheric effect was most efficient in disentangling ADD/DLB and PDD at the group level.

Another finding was the discriminant intrahemispheric LLC patterns ADD < DLB and PDD < Nold, fitted only by the frontal alpha 2 sources ($p < 0.05$ to 0.00001). These discriminant LLC solutions exhibited a very marked reduction in the ADD group ($p <$ 0.00001), whereas the decrease was moderate in the DLB and PDD groups ($p < 0.05$). This was the only intrahemispheric effect differentiating ADD and DLB at the group level.

Finally, intrahemispheric LLC solutions in the temporal delta sources were higher in the ADD than the Nold, PDD, and DLB groups ($p < 0.05$ to 0.005). In addition, intrahemispheric LLC solutions in the frontal, central, parietal, and occipital delta sources were higher in the ADD than the Nold group ($p < 0.01$ to 0.0001).

A control statistical analysis was performed to verify that the aforementioned discriminant LLC solutions were not merely due to some outliers. To this aim, the Grubbs' test ($p < 0.0001$) tested the presence of outliers in the data of the 4 groups (i.e., Nold, ADD, DLB, and PDD). The analysis was performed for the 6 discriminant

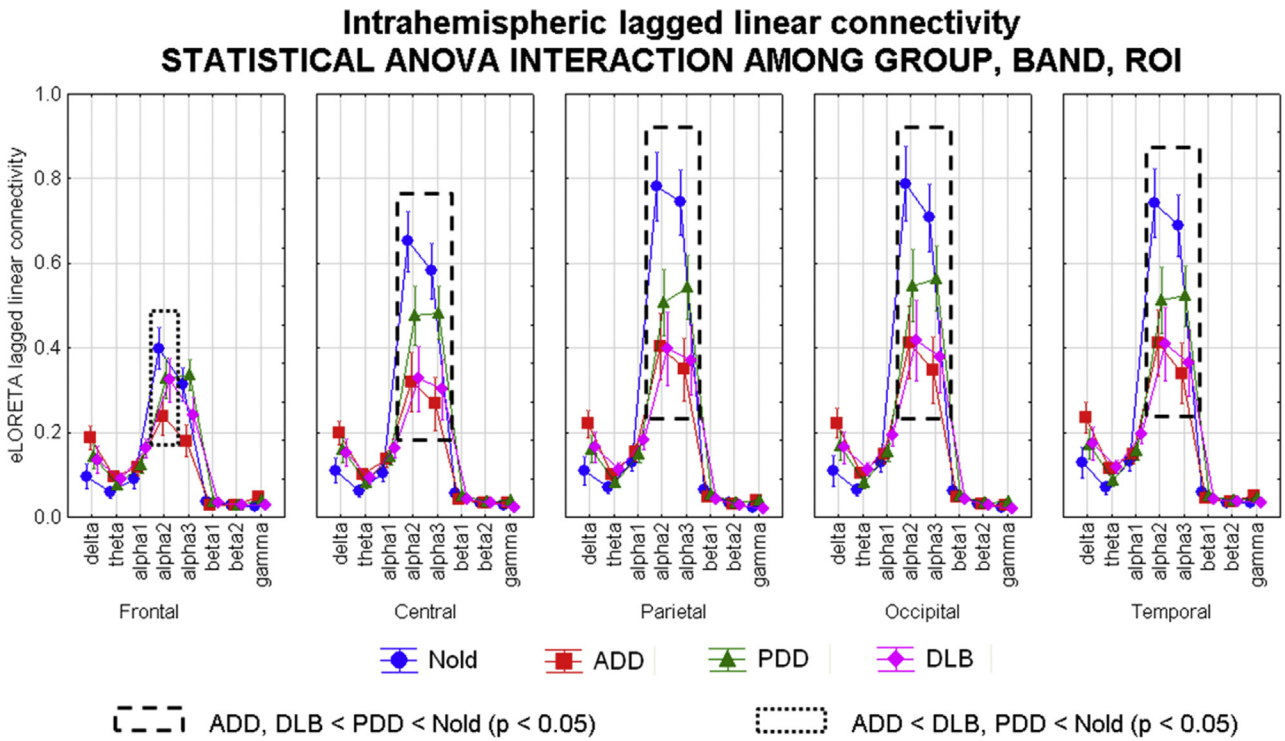

Fig. 3. Mean values (±SE) of the intrahemispheric LLC solutions computed in eLORETA cortical sources of rsEEG rhythms relative to a statistically significant ANOVA interaction effect ($F = 5.4$, $p < 0.0001$) among the factors Group (Nold, ADD, PDD, and DLB), Band (delta, theta, alpha 1, alpha 2, alpha 3, beta 1, beta 2, and gamma), and ROI (frontal, central, parietal, occipital, and temporal). The rectangles indicate the ROIs and frequency bands in which the intrahemispheric LLC solutions presented statistically significant differences among the four groups of participants ($p < 0.05$). Abbreviations: ADD, Alzheimer's disease with dementia; ANOVA, analysis of variance; DLB, Lewy body dementia; eLORETA, exact low-resolution brain electromagnetic tomography; LLC, lagged linear connectivity; PDD, Parkinson's disease with dementia; rsEEG, resting-state eyes-closed electroencephalographic; SE, standard error of the mean.

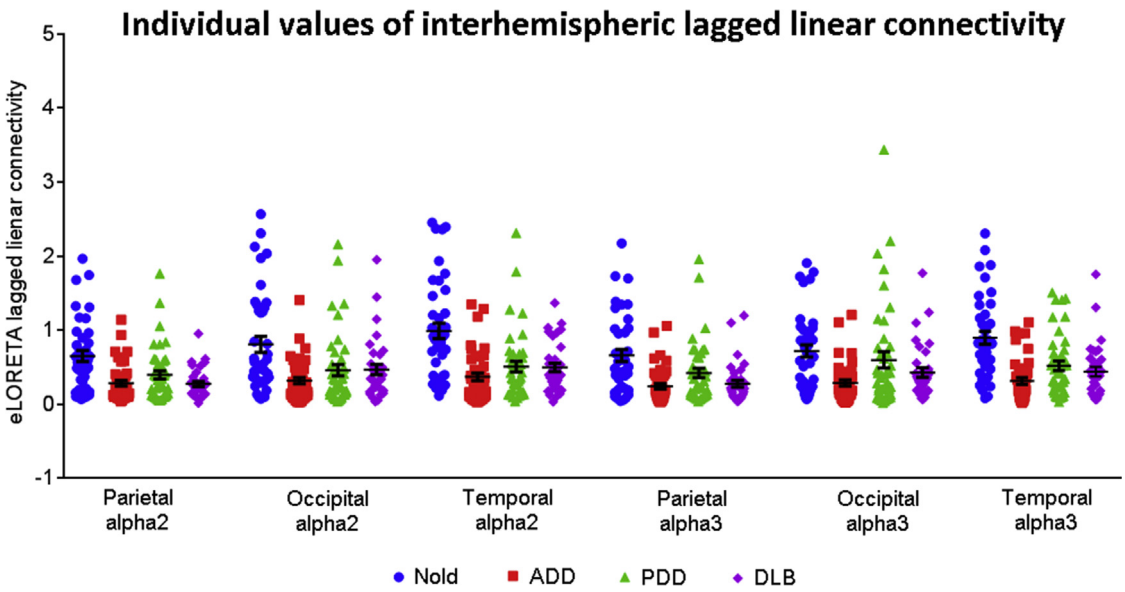

Fig. 4. Individual values of the interhemispheric LLC solutions computed in eLORETA cortical sources of alpha rhythms showing statistically significant ($p < 0.05$) differences between the Nold, ADD, PDD, and DLB groups (i.e., parietal, occipital, and temporal alpha 2; parietal, occipital, and temporal alpha 3). Noteworthy, the Grubbs' test showed no outliers from those individual values of the interhemispheric LLC solutions (arbitrary threshold of $p < 0.0001$). Abbreviations: ADD, Alzheimer's disease with dementia; DLB, Lewy body dementia; eLORETA, exact low-resolution brain electromagnetic tomography; LLC, lagged linear connectivity; Nold, normal healthy older; PDD, Parkinson's disease with dementia.

interhemispheric LLC solutions in the alpha sources (i.e., parietal, occipital, and temporal alpha 2; parietal, occipital, and temporal alpha 3) and the 9 discriminant intrahemispheric LLC solutions in those sources (i.e., frontal, central, parietal, occipital, and temporal alpha 2; central, parietal, occipital, and temporal alpha 3). Furthermore, this analysis was also performed for 1 interhemispheric LLC solution in the occipital delta sources and 5 intrahemispheric LLC solutions in the frontal, central, parietal, occipital, and temporal delta sources. No outlier was found in any group (see Figs. 4 and 5), thus confirming the results of the main statistical analysis.

3.4. Correlation of LLC solutions and MMSE scores across Nold, ADD, DLB, and PDD individuals

As a first exploratory analysis at the individual level, the Spearman test evaluated the correlation between the MMSE score and 21 LLC solutions showing statistically significant differences between the Nold and the patients' groups ($p < 0.05$). These LLC solutions are listed in the following: (1) interhemispheric LLC solutions in the occipital delta sources; (2) interhemispheric LLC solutions in the parietal, occipital, and temporal alpha 2 sources; (3) interhemispheric LLC solutions in the parietal, occipital, and

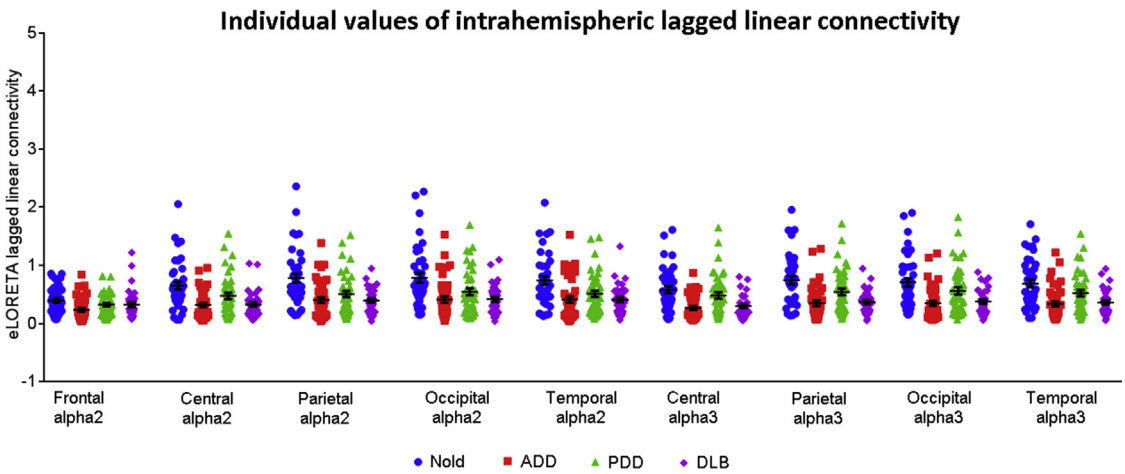

Fig. 5. Individual values of the intrahemispheric LLC solutions computed in eLORETA cortical sources of alpha rhythms showing statistically significant ($p < 0.05$) differences between the Nold, ADD, PDD, and DLB groups (i.e., frontal, central, parietal, occipital, and temporal alpha 2; central, parietal, occipital, and temporal alpha 3). Noteworthy, the Grubbs' test showed no outliers from those individual values of the intrahemispherical LLC of eLORETA rsEEG cortical sources (arbitrary threshold of $p < 0.0001$). Abbreviations: ADD, Alzheimer's disease with dementia; DLB, Lewy body dementia; eLORETA, exact low-resolution brain electromagnetic tomography; LLC, lagged linear connectivity; PDD, Parkinson's disease with dementia; rsEEG, resting-state eyes-closed electroencephalographic.

temporal alpha 3 sources; (4) intrahemispheric LLC solutions in the frontal, central, parietal, occipital, and temporal delta sources; (5) intrahemispheric LLC solutions in the frontal, central, parietal, occipital, and temporal alpha 2 sources; and (6) intrahemispheric LLC solutions in the central, parietal, occipital, and temporal alpha 3 sources. To take into account the inflating effects of repetitive univariate tests, the statistical threshold was set at $p < 0.0023$ to obtain the Bonferroni correction at $p < 0.05$.

A positive correlation was found between the interhemispheric LLC solutions in the temporal alpha 3 sources and the MMSE scores ($r = 0.24$, $p < 0.002$); the lower the interhemispheric LLC solutions, the lower the MMSE score. Similarly, the intrahemispheric LLC solutions in the central ($r = 0.26$, $p < 0.001$), parietal ($r = 0.26$, $p < 0.001$), and occipital ($r = 0.26$, $p < 0.002$) alpha 3 sources were correlated with the MMSE scores; the lower the intrahemispheric LLC solutions, the lower the MMSE scores. Fig. 6 shows the scatter plots of those 4 LLC solutions showing statistically significant correlations ($p < 0.05$ corrected).

The LLC solutions in the delta sources showed only marginal statistical effects. There was a significant negative correlation between the interhemispheric occipital delta sources and the MMSE score ($r = -0.21$; $p = 0.005$). The higher the interhemispheric LLC solutions in those sources, the lower the MMSE score.

As a control analysis, the same correlation test was performed for any single group considered separately. No statistically significant result ($p > 0.05$) was observed, possibly due to the limited range of the MMSE score within the single groups.

3.5. Classification among Nold, ADD, PDD, and DLB individuals based on the discriminant LLC solutions

As a second exploratory analysis at the individual level, the aforementioned 15 LLC solutions showing statistically significant differences between the Nold and the 3 patients' groups ($p < 0.05$) were used as an input to the computation of the AUROC curves. In addition, this analysis was also performed for 1 interhemispheric LLC solution in the occipital delta sources and 5 intrahemispheric LLC solutions in the frontal, central, parietal, occipital, and temporal delta sources for the classification of the Nold and ADD individuals. This second exploratory analysis tested the ability of those LLC solutions in the classification of (1) Nold participants versus patients and (2) patients of 2 paired pathological groups (i.e., ADD vs. DLB, ADD vs. PDD, and DLB vs. PDD). Maximum classification accuracies were obtained in the classification between the Nold participants and ADD patients and between the Nold and DLB patients. Table 4 reports the results in detail.

The classification between Nold versus ADD individuals showed that all 15 LLC solutions in the alpha sources overcome the threshold of 0.7 of the AUROC curve (i.e., the inferior limit of a "moderate" classification rate). Among these LLC solutions, the

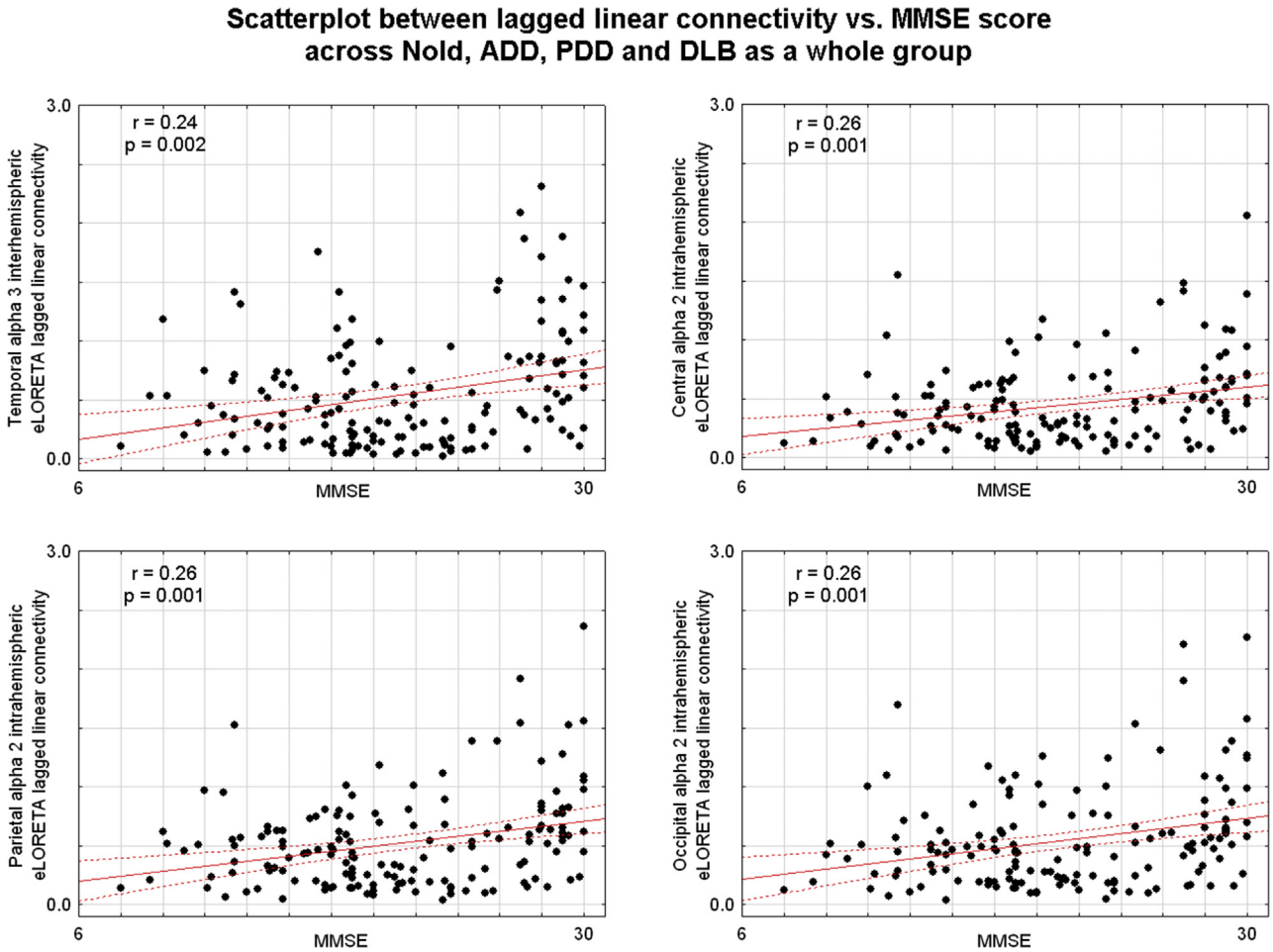

Fig. 6. Scatter plots showing the correlation between LLC solutions computed in eLORETA cortical sources of alpha rhythms and the MMSE score in the Nold, ADD, PDD, and DLB participants as a whole group. The Spearman test evaluated the hypothesis of that correlation (Bonferroni correction at $p < 0.05$). The r and p values are reported within the diagram. Abbreviations: ADD, Alzheimer's disease with dementia; DLB, Lewy body dementia; eLORETA, exact low-resolution brain electromagnetic tomography; LLC, lagged linear connectivity; Nold, normal healthy older; PDD, Parkinson's disease with dementia.

Table 4
Results of the classification among Nold, ADD, PDD, and DLB individuals based on the LLC solutions computed in eLORETA cortical sources of rsEEG rhythms at individual delta and alpha frequency bands

Classification of Nold, ADD, PDD, and DLB individuals based on lagged linear connectivity of rsEEG cortical sources					
	Lagged linear connectivity (LLC)	Sensitivity (%)	Specificity (%)	Accuracy (%)	AUROC
Nold vs. ADD	Occipital delta interhemispheric	61.9	77.5	69.7	0.70
	Parietal alpha 2 interhemispheric	83.3	67.5	75.4	0.76
	Occipital alpha 2 interhemispheric	61.9	80	71	0.74
	Temporal alpha 2 interhemispheric	85.7	67.5	76.6	0.81
	Parietal alpha 3 interhemispheric	73.8	72.5	73.2	0.79
	Occipital alpha 3 interhemispheric	88.1	62.5	75.3	0.77
	Temporal alpha 3 interhemispheric	78.6	77.5	78.1	0.84
	Frontal alpha 2 intrahemispheric	57.1	85.0	71.1	0.73
	Central alpha 2 intrahemispheric	69.1	82.5	75.8	0.77
	Parietal alpha 2 intrahemispheric	71.4	77.5	74.5	0.77
	Occipital alpha 2 intrahemispheric	69.1	80.0	74.5	0.75
	Temporal alpha 2 intrahemispheric	69.1	80.0	74.5	0.74
	Central alpha 3 intrahemispheric	64.3	87.5	75.9	0.79
	Parietal alpha 3 intrahemispheric	61.9	87.5	74.7	0.79
	Occipital alpha 3 intrahemispheric	64.3	82.5	73.4	0.77
	Temporal alpha 3 intrahemispheric	47.6	95.0	71.3	0.77
Nold vs. PDD	**Temporal alpha 2 interhemispheric**	**82.3**	**70**	**76.2**	**0.75**
	Temporal alpha 3 interhemispheric	73.8	65	69.4	0.72
Nold vs. DLB	Parietal alpha 2 interhemispheric	82.4	67.5	74.9	0.76
	Temporal alpha 2 interhemispheric	76.5	67.5	72	0.72
	Parietal alpha 3 interhemispheric	79.4	70.0	74.7	0.75
	Temporal alpha 3 interhemispheric	91.2	57.5	74.3	0.77
	Central alpha 2 intrahemispheric	**83.5**	**65**	**74.3**	**0.78**
	Parietal alpha 2 intrahemispheric	73.5	77.5	75.5	0.77
	Occipital alpha 2 intrahemispheric	70.6	75.0	72.8	0.75
	Temporal alpha 2 intrahemispheric	85.3	57.5	71.4	0.74
	Central alpha 3 intrahemispheric	73.5	72.5	73.0	0.76
	Parietal alpha 3 intrahemispheric	94.1	60.0	77.1	0.77
	Occipital alpha 3 intrahemispheric	70.6	70.0	70.3	0.74
	Temporal alpha 3 intrahemispheric	76.5	65.0	70.7	0.75

These LLC solutions were those showing statistically significant differences among the 4 groups (i.e., Nold, ADD, PDD, and DLB) in the main statistical analysis. The classification rate is computed by the analysis of the AUROC curve. The table reports the classification indexes (sensitivity, specificity, and accuracy) for all the LLC solutions in delta and alpha sources having a value higher than 0.70 in the AUROC curves. The best classification results for each LLC solution in the classifications of interest, namely Nold versus ADD individuals, Nold versus DLB individuals, and Nold versus PDD individuals, are in bold.
Key: ADD, Alzheimer's disease with dementia; AUROC, area under receiver operating characteristic; DLB, Lewy body dementia; eLORETA, exact low-resolution brain electromagnetic tomography; LLC, lagged linear connectivity; Nold, normal healthy older; PDD, Parkinson's disease with dementia; rsEEG, resting-state electroencephalographic.

interhemispheric temporal alpha 3 LLC solutions reached the following best classification rate (Fig. 7 top): a sensitivity of 78.6%, a specificity of 77.5%, an accuracy of 78.1%, and 0.84 of the AUROC curve. Among the LLC solutions of the delta sources, only the interhemispheric occipital delta LLC solutions reached the threshold of 0.7 of the AUROC curve. It was observed a sensitivity of 61.9%, a specificity of 77.5%, an accuracy of 69.8%, and 0.70 of the AUROC curve.

Concerning the classification of the Nold versus PDD individuals, only the following 2 LLC solutions in alpha sources overcome the threshold of 0.7 of the AUROC curve (Table 4): interhemispheric LLC solutions in the temporal alpha 2 and alpha 3 sources. Among these LLC solutions, the interhemispheric LLC solutions in the temporal alpha 2 sources reached the following best classification rate (Fig. 7, middle): a sensitivity of 82.3%, a specificity of 70%, an accuracy of 76.2%, and 0.75 of the AUROC curve.

Regarding the classification of the Nold versus DLB individuals, the following 12 LLC solutions in alpha sources overcome the threshold of 0.7 of the AUROC curve (Table 4): (1) interhemispheric LLC solutions in the parietal alpha 2, temporal alpha 2, parietal alpha 3, and temporal alpha 3 sources and (2) intrahemispheric LLC solutions in the central alpha 2, parietal alpha 3, temporal alpha 2, occipital alpha 2, central alpha 3, parietal alpha 3, occipital alpha 3, and temporal alpha 3 sources. Among these LLC solutions, the intrahemispheric 2 LLC solutions in the central alpha sources reached the following best classification rate (Fig. 7, bottom): a sensitivity of 83.5%, a specificity of 65%, an accuracy of 74.3%, and 0.78 of the AUROC curve.

3.6. Control analysis

As mentioned previously, head volume conduction and "common drive/source" on EEG signals may mislead estimates (especially "bivariate") of functional connectivity inducing a number of "false" connections between pairs of scalp sensors or source solutions. Typically, these "false" connections are characterized by a "random" spatial topology. Keeping in mind the considerations, we performed a control analysis focused on the alpha sources (a relevant EEG frequency band in the present study) aimed at testing the hypotheses that (1) the present LLC solutions did not show a "random" spatial scheme between the pairs of ROIs in the Nold group and (2) the statistical differences in the alpha LLC solutions between the Nold group and the ADD, PDD, or DLB group did not show a "random" spatial scheme between the ROI pairs. To test these hypotheses, we used the following ANOVA designs with LLC solutions between pairs of ROIs as a dependent variable. The post hoc analysis compared the LLC solutions for between the pairs of ROIs using a liberal threshold of $p < 0.05$ allowing a "random" topology of the functional connections to emerge, if present.

The first control ANOVA design was focused on the alpha LLC solutions of the Nold group ($p < 0.05$). The ANOVA factors were Band (alpha 2 and alpha 3) and Pair of ROIs (frontal-central, frontal-temporal, central-temporal, frontal-parietal, central-parietal, temporal-parietal, frontal-occipital, central-occipital, temporal-occipital, and parietal-occipital). The results showed a significant main effect for the factor Pair of ROIs ($F = 35.9$, $p < 0.00001$), regardless the alpha sub-bands. The Duncan post hoc analysis

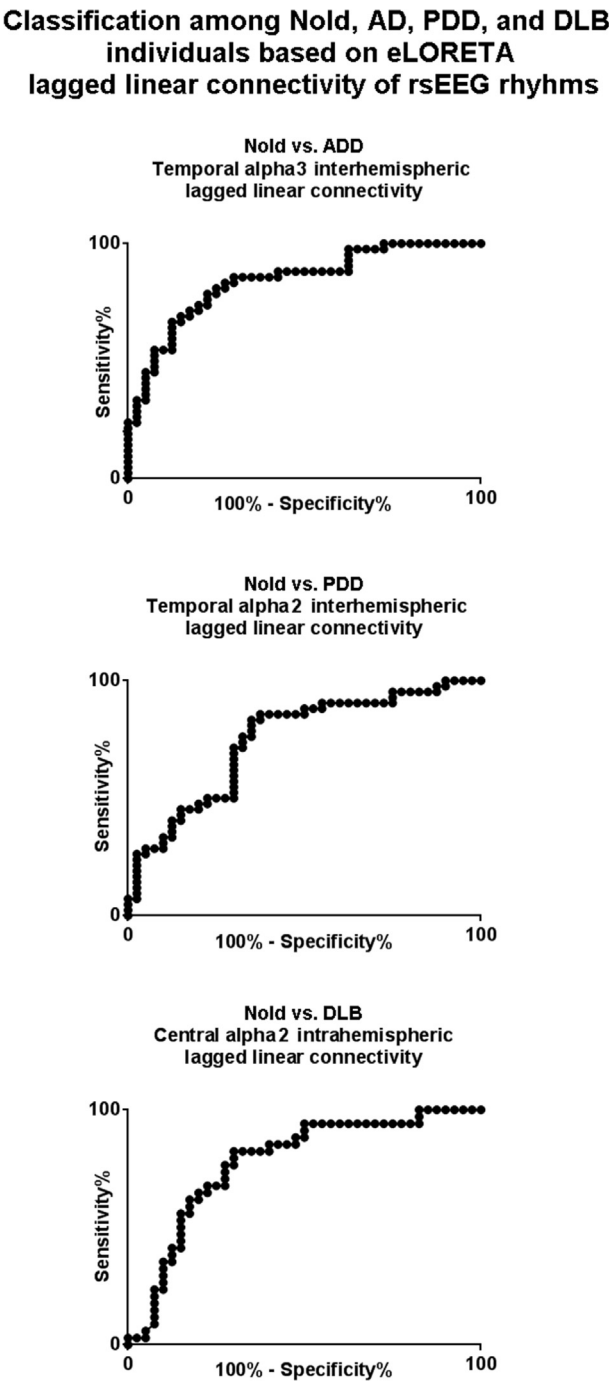

Fig. 7. (Top): ROC curve illustrating the classification of the ADD and Nold individuals based on the interhemispheric LLC solutions computed in temporal alpha 2 cortical sources. The AUROC curve was 0.84 (e.g., 1 = 100%), indicating a good classification accuracy for the ADD and Nold individuals. (Middle): The ROC curve illustrating the classification of the PDD and Nold individuals based on the interhemispheric LLC solutions computed in temporal alpha 3 cortical sources. The AUROC was 0.72, indicating a moderate classification accuracy of the PDD and Nold individuals. (Bottom): The ROC curve illustrating the classification of the DLB and Nold individuals based on the intrahemispheric LLC solutions computed in central alpha 2 cortical sources. The AUROC was 0.78, indicating a moderate classification accuracy of the DLB and Nold individuals. Abbreviations: ADD, Alzheimer's disease with dementia; AUROC, area under receiver operating characteristic; DLB, Lewy body dementia; LLC, lagged linear connectivity; Nold, normal healthy older; PDD, Parkinson's disease with dementia; ROC, receiver operating characteristic.

showed a characteristic topology of the pairs of ROIs exhibiting the greatest effects. For example, the parietal-occipital alpha LLC solutions were higher than those in the temporal-occipital ($p < 0.00001$), temporal-parietal ($p < 0.00005$), central-parietal ($p < 0.00001$), central-temporal ($p < 0.00001$), frontal-temporal ($p < 0.00001$), and frontal-central ($p < 0.00001$), despite a similar spatial distance between the ROIs in those pairs. In the same line, the temporal-parietal alpha LLC solutions were higher than those in the frontal-temporal ($p < 0.00001$) and frontal-central ($p < 0.00001$), despite a similar spatial distance between the ROIs in those pairs. Fig. 8A and Table 5 report all details of the results of the first control ANOVA design. These results are not in line with a "random" topology of the functional connections.

The second control ANOVA design was focused on the alpha LLC solutions in the comparison between the Nold and the ADD group ($p < 0.05$). The ANOVA factors were Group (Nold and ADD), Band (alpha 2 and alpha 3), and Pair of ROIs (frontal-central, frontal-temporal, central-temporal, frontal-parietal, central-parietal, temporal-parietal, frontal-occipital, central-occipital, temporal-occipital, and parietal-occipital). The results showed a significant interaction Group × Pair of ROIs ($F = 5.7$, $p < 0.00001$), regardless the alpha sub-bands. The Duncan post hoc analysis showed a characteristic topology of the pairs of ROIs having the highest values of alpha LLC solutions in the ADD group. For example, the parietal-occipital alpha LLC solutions were higher than those in the frontal-central ($p < 0.00001$) and central-temporal ($p < 0.0001$) pairs of ROIs, despite a similar spatial distance between the ROIs in those pairs. The Duncan post hoc analysis also showed the pairs of ROIs exhibiting the significant differences in the alpha LLC solutions between the Nold and the ADD group. Compared with the Nold group, the ADD group showed lower alpha LLC solutions in frontal-temporal, central-temporal, central-parietal, temporal-parietal, central-occipital, temporal-occipital, and parietal-occipital pairs of ROIs ($p < 0.005$ to 0.000001). Among them, a clear topology emerged. For example, the differences were higher in the parietal-occipital ($p < 0.00001$) than the temporal-parietal ($p < 0.0005$), temporo-occipital ($p < 0.001$), frontal-temporal ($p < 0.005$), and frontal-central (n.s.) pairs of ROIs. Fig. 8B reports all details of the results of the second control ANOVA design. These results are not in line with a "random" topology of the differences in the functional connections between the Nold and the ADD group.

The third control ANOVA design was focused on the alpha LLC solutions in the comparison between the Nold and the PDD group ($p < 0.05$). The ANOVA factors were Group (Nold and PDD), Band (alpha 2 and alpha 3), and Pair of ROIs (frontal-central, frontal-temporal, central-temporal, frontal-parietal, central-parietal, temporal-parietal, frontal-occipital, central-occipital, temporal-occipital, and parietal-occipital). The results showed a significant interaction Group × Pair of ROIs ($F = 2.5$, $p < 0.01$), regardless the alpha sub-bands. The Duncan post hoc analysis showed a characteristic topology of the pairs of ROIs having the highest values of alpha LLC solutions in the PDD group. For example, the parietal-occipital alpha LLC solutions were higher than those in the parietal-temporal ($p < 0.01$) pairs of ROIs, despite a similar spatial distance between the ROIs in those pairs. In the same line, the central-parietal alpha LLC solutions were higher than those in the frontal-central ($p < 0.00001$) and frontal-parietal ($p < 0.00001$) pairs of ROIs. The Duncan post hoc analysis also showed a characteristic topology of the pairs of ROIs exhibiting the significant differences in the alpha LLC solutions between the Nold and the PDD group ($p < 0.05$). Compared with the Nold group, the PDD group showed lower alpha LLC solutions only in the central-temporal,

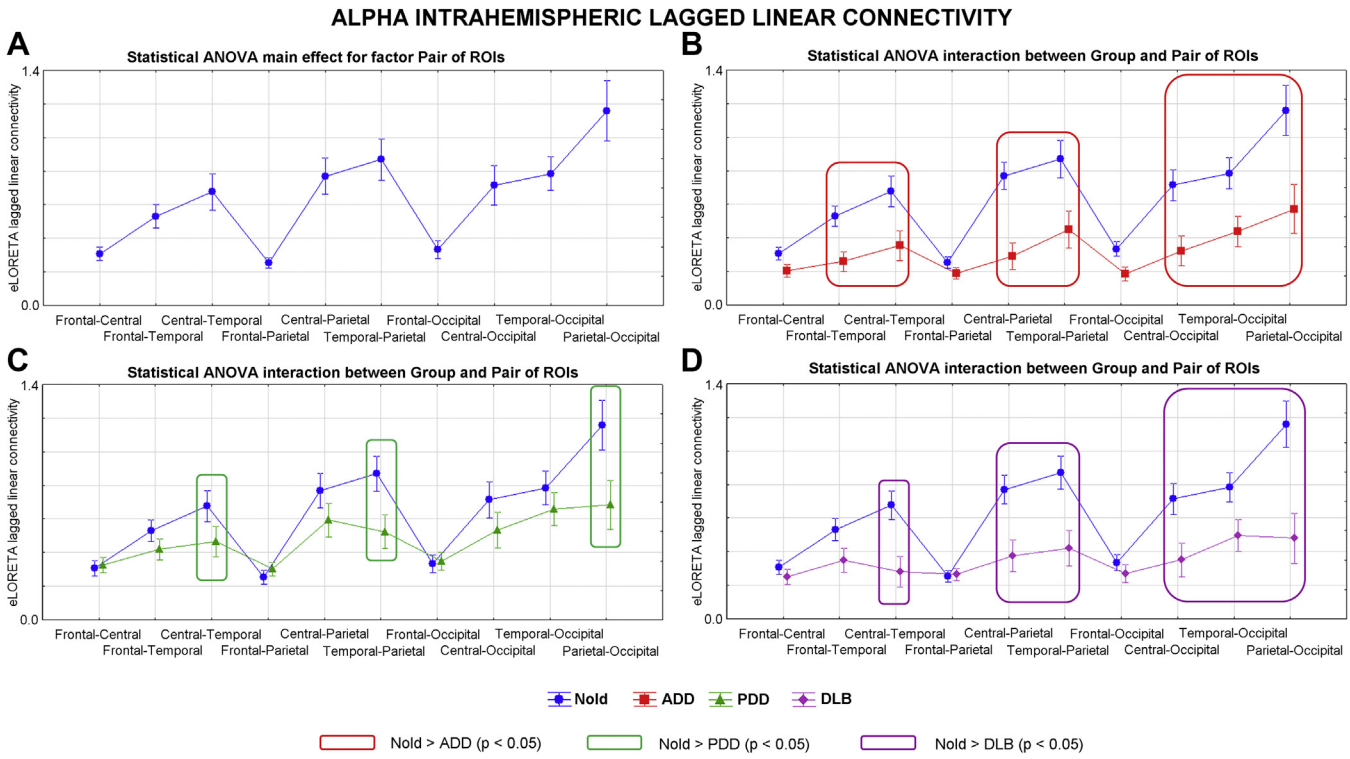

Fig. 8. (A): Mean values (±SE) of the intrahemispheric LLC solutions computed in eLORETA cortical sources of alpha rsEEG rhythms relative to a statistically significant main effect ($F = 35.9$, $p < 0.00001$) for the factor Pair of ROIs (frontal-central, frontal-temporal, central-temporal, frontal-parietal, central-parietal, temporal-parietal, frontal-occipital, central-occipital, temporal-occipital, and parietal-occipital) in Nold participants. (B): Mean values (±SE) of the intrahemispheric LLC solutions computed in eLORETA cortical sources of alpha rsEEG rhythms relative to a statistically significant ANOVA interaction effect ($F = 5.7$, $p < 0.00001$) among the factors Group (Nold and ADD) and Pair of ROIs (frontal-central, frontal-temporal, central-temporal, frontal-parietal, central-parietal, temporal-parietal, frontal-occipital, central-occipital, temporal-occipital, and parietal-occipital). The rectangles indicate the pair of ROIs in which the intrahemispheric LLC solutions presented statistically significant differences between Nold and ADD groups ($p < 0.05$). (C): Mean values (±SE) of the intrahemispheric LLC solutions computed in eLORETA cortical sources of alpha rsEEG rhythms relative to a statistically significant ANOVA interaction effect ($F = 2.5$, $p < 0.01$) among the factors Group (Nold and PDD) and Pair of ROIs (frontal-central, frontal-temporal, central-temporal, frontal-parietal, central-parietal, temporal-parietal, frontal-occipital, central-occipital, temporal-occipital, and parietal-occipital). The rectangles indicate the pair of ROIs in which the intrahemispheric LLC solutions presented statistically significant differences between Nold and PDD groups ($p < 0.05$). (D): Mean values (±SE) of the intrahemispheric LLC solutions computed in eLORETA cortical sources of alpha rsEEG rhythms relative to a statistically significant ANOVA interaction effect ($F = 4.2$, $p < 0.00005$) among the factors Group (Nold and DLB) and Pair of ROIs (frontal-central, frontal-temporal, central-temporal, frontal-parietal, central-parietal, temporal-parietal, frontal-occipital, central-occipital, temporal-occipital, and parietal-occipital). The rectangles indicate the pair of ROIs in which the intrahemispheric LLC solutions presented statistically significant differences between Nold and DLB groups ($p < 0.05$). Abbreviations: ADD, Alzheimer's disease with dementia; ANOVA, analysis of variance; DLB, Lewy body dementia; eLORETA, exact low-resolution brain electromagnetic tomography; LLC, lagged linear connectivity; Nold, normal healthy older; PDD, Parkinson's disease with dementia; ROI, region of interest; rsEEG, resting-state eyes-closed electroencephalographic; SE, standard error mean.

central-parietal, temporal-parietal, and parietal-occipital pairs of ROIs ($p < 0.05$ to 0.00001). Fig. 8C reports all details of the results of the third control ANOVA design. These results are not in line with a "random" topology of the differences in the functional connections between the Nold and the PDD group.

The fourth control ANOVA design was focused on the alpha LLC solutions in the comparison between the Nold and the DLB group ($p < 0.05$). The ANOVA factors were Group (Nold and DLB), Band (alpha 2 and alpha 3), and Pair of ROIs (frontal-central, frontal-temporal, central-temporal, frontal-parietal, central-parietal, temporal-parietal, frontal-occipital, central-occipital, temporal-occipital, and parietal-occipital). The results showed a significant interaction Group × Pair of ROIs ($F = 4.2$, $p < 0.00005$), regardless the alpha sub-bands. The Duncan post hoc analysis showed a characteristic topology of the pairs of ROIs having the highest values of alpha LLC solutions in the DLB group. For example, the parietal-occipital alpha LLC solutions were higher than those in the central-temporal ($p < 0.001$) and frontal-central ($p < 0.0005$) pairs of ROIs, despite a similar spatial distance between the ROIs in those pairs. The Duncan post hoc analysis also showed a characteristic topology of the pairs of ROIs exhibiting the significant differences in the alpha LLC solutions between the Nold and the DLB group ($p < 0.05$). Compared with the Nold group, the DLB group showed lower alpha LLC solutions in the central-temporal, central-parietal, temporal-parietal, central-occipital, temporal-occipital, and parietal-occipital ($p < 0.005$ to 0.000001). Among them, a clear topology emerged. For example, the differences were higher in the parietal-occipital ($p < 0.000001$) than the temporal-parietal ($p < 0.00001$), temporo-occipital ($p < 0.005$), frontal-central (n.s.), and frontal-temporal (n.s.) pairs of ROIs, despite a similar spatial distance between the ROIs in those pairs. Fig. 8D reports all details of the results of the third control ANOVA design. These results are not in line with a "random" topology of the differences in the functional connections between the Nold and the DLB group.

4. Discussion

In the present exploratory investigation, we reanalyzed the rsEEG data of a previous reference study (Babiloni et al., 2017) to test the core hypothesis that ADD patients might show the maximum abnormality of "functional cortical connectivity" compared with DLB and PDD patients, leading support to the idea of AD as a "cortical disconnection syndrome", intrahemispherically and interhemispherically (Besthorn et al., 1994; Bokde et al., 2009; Dunkin et al., 1995; Leuchter et al., 1994; Reuter-Lorenz and Mikels, 2005; Teipel et al., 2016). The data reanalysis was performed

Table 5
Duncan post hoc relative to a statistically significant main effect ($F = 35.9$, $p < 0.00001$) for the factor Pair of ROIs (frontal-central, frontal-temporal, central-temporal, frontal-parietal, central-parietal, temporal-parietal, frontal-occipital, central-occipital, temporal-occipital, and parietal-occipital) in an ANOVA design focused on the intrahemispheric LLC solutions computed in eLORETA cortical sources of alpha rsEEG rhythms of the Nold group ($p < 0.05$)

	Frontal-central	Frontal-temporal	Central-temporal	Frontal-parietal	Central-parietal	Temporal-parietal	Frontal-occipital	Central-occipital	Temporal-occipital	Parietal-occipital
Frontal-central		<0.001	<0.00001	n.s.	<0.00001	<0.00001	n.s.	<0.00001	<0.00001	<0.00001
Frontal-temporal	<0.001		<0.05	<0.0001	<0.001	<0.00001	<0.005	<0.01	<0.0005	<0.00001
Central-temporal	<0.00001	<0.05		<0.00001	n.s	<0.01	<0.00001	n.s	n.s	<0.00001
Frontal-parietal	n.s.	<0.0001	<0.00001		<0.00001	<0.00001	n.s	<0.00001	<0.00001	<0.00001
Central-parietal	<0.00001	<0.001	n.s	<0.00001		n.s	<0.00001	n.s	n.s	<0.00001
Temporal-parietal	<0.00001	<0.00001	<0.01	<0.00001	n.s		<0.00001	n.s	n.s	<0.00005
Frontal-occipital	n.s.	<0.005	<0.00001	n.s	<0.00001	<0.00001		<0.00001	<0.00001	<0.00001
Central-occipital	<0.00001	<0.01	n.s	<0.00001	n.s	n.s	<0.00001		n.s	<0.00001
Temporal-occipital	<0.00001	<0.0005	n.s	<0.00001	n.s	n.s	<0.00001	n.s		<0.00001
Parietal-occipital	<0.00001	<0.00001	<0.00001	<0.00001	<0.00001	<0.00005	<0.00001	<0.00001	<0.00001	

Key: ANOVA, analysis of variance; eLORETA, exact low-resolution brain electromagnetic tomography; LLC, lagged linear connectivity; n.s., not significant; Nold, normal healthy older; ROI, region of interest; rsEEG, resting-state eyes-closed electroencephalographic.

computing the interhemispheric and intrahemispheric (eLORETA) LLC solutions in cortical sources of rsEEG rhythms at individually selected frequency bands. The results are summarized and discussed in the following sections.

4.1. The functional cortical connectivity in alpha sources was maximally abnormal in the AD group

In the Nold group as a physiological reference, interhemispheric and intrahemispheric LLC solutions were dominant in posterior alpha sources, suggesting a possible strict relationship of this extensive posterior functional connectivity with the prominent local activation of the same alpha sources, previously reported from the same database (Babiloni et al., 2017). Compared with the Nold group, the decrement of LLC solutions in alpha sources was dramatic in the ADD group, marked in the DLB group, and moderate in the PDD group. Furthermore, the intrahemispheric LLC solutions in widespread alpha sources exhibited a greater reduction in both ADD and DLB groups when compared with the PDD group. Finally, the LLC solutions in frontal alpha sources pointed to a very marked reduction in the ADD group compared with the moderate decrease found in both DLB and PDD groups.

On one hand, these findings might reflect similarities and differences in cortical neuropathology and clinical features among ADD, DLB, and PDD. This similarity was observed between ADD and DLB in a recent retrospective study based on data from 213 patients receiving a diagnosis of DLB and α synucleinopathy confirmed by brain autopsy (Irwin et al., 2017). There were 23% patients with no AD neuropathology, 26% with low-level AD neuropathology, 21% with intermediate-level AD neuropathology, and 30% with high-level AD neuropathology (Irwin et al., 2017). Furthermore, the increased AD neuropathology was associated with higher cerebral α-synuclein scores and a shorter interval between the onset of motor or dementia symptoms and the death (Irwin et al., 2017). In another study, about 25% of DLB patients and 9% of PDD patients had abnormal CSF values for t-tau, $A\beta_{42}$, and p-tau, thus suggesting that a CSF profile of AD is more common in DLB compared with PDD patients (van Steenoven et al., 2016). Moreover, there was evidence that compared with DLB patients with AD neuropathology, DLB patients without AD neuropathology showed greater impairment on visuospatial constructions, visual conceptual reasoning, the speed of processing, and more frequent hallucinations, but less impairment of confrontation naming and verbal memory (Peavy et al., 2016). Finally, compared with DLB patients negative to pathophysiological $A\beta_{42}$ and tau markers in CSF, DLB patients positive to those markers showed a greater decline in the MMSE score (Abdelnour et al., 2016).

The present evidence of a common frontal effect in the DLB and PDD groups might be explained by the partially common neuropathology of subcortical projection to the frontal lobe and similar clinical features in the 2 diseases (Barker and Williams-Gray, 2016). Both these neurodegenerative dementing disorders share characteristic neuropathological changes including deposition of α-synuclein in Lewy bodies and neurites, loss of tegmental dopamine cell populations, loss of basal forebrain cholinergic projection to the cortex, and a variable degree of coexisting AD neuropathology (Irwin et al., 2017). Clinical constellations of both DLB and PDD include progressive cognitive impairment associated with parkinsonism, visual hallucinations, frontal executive dysfunctions, and fluctuations of attention and wakefulness (Barker and Williams-Gray, 2016).

The present results extend to source space and individually determined frequency bands previous EEG evidence showing differences in the functional cortical connectivity estimated from scalp rsEEG rhythms in ADD, PDD, and DLB groups compared with Nold

participants (Adler et al., 2003; Andersson et al., 2008; Anghinah et al., 2000; Besthorn et al., 1994; Dunkin et al., 1994; Fonseca et al., 2011, 2013; Jelic et al., 1997, 2000; Knott et al., 2000; Leuchter et al., 1987, 1992; Locatelli et al., 1998; Moazami-Goudarzi et al., 2008; Pogarell et al., 2005; Sloan et al., 1994; van Dellen et al., 2015). In previous studies, ADD patients were characterized by lower functional cortical connectivity computed from posterior alpha (8–12 Hz) and beta (13–20 Hz) rhythms, but the topographical regional localization of the effects was not consistent across the investigations with the exception of a prominent anterior-posterior axis of the connectivity alteration (Adler et al., 2003; Anghinah et al., 2000; Babiloni et al., 2004, 2006b, 2016b; Besthorn et al., 1994; Blinowska et al., 2017; Dunkin et al., 1994; Fonseca et al., 2011, 2013; Jelic et al., 1997, 2000; Knott et al., 2000; Leuchter et al., 1987, 1992; Locatelli et al., 1998; Pogarell et al., 2005; Sloan et al., 1994). Similarly, the present results extend as spatial and frequency specifications the previous evidence of abnormalities of the interhemispheric and intrahemispheric scalp frontoparietal alpha coherences in PD patients with cognitive deficits (Fonseca et al., 2013; Teramoto et al., 2016) and DLB participants (Dauwan et al., 2016a).

Previous investigations in animals have delineated an interesting model of the generation of cortical alpha rhythms in quiet wakefulness (Hughes and Crunelli, 2005; Lörincz et al., 2008, 2009). These rhythms might result from a physiological neurotransmission between populations of cortical pyramidal, thalamocortical, and reticular thalamic neurons (Hughes and Crunelli, 2005; Lörincz et al., 2008, 2009). Alpha rhythms in that thalamocortical network may produce cycles of neuronal excitation and inhibition that might frame perceptual events in discrete snapshots of around 70–100 ms during active sensory and motor information processing (Hughes and Crunelli, 2005; Lörincz et al., 2008, 2009). In this line, the present evidence of reduced alpha source connectivity in patients with dementia, especially in ADD participants, might be due to a downregulation of that neurophysiological mechanism. As a result, an unselective tonic cortical excitation might occur in quiet wakefulness. Such cortical overexcitation could represent a sort of background noise, possibly interfering with the switch of the cerebral cortex from quiet wakefulness to focused attention and local adaptive encoding and retrieval information processing when required by endogenous or external demands (Babiloni et al., 2016a).

4.2. The functional cortical connectivity in delta sources was abnormal only in the AD group

Here, we report the negligible magnitude of the interhemispheric and intrahemispheric LLC solutions in delta sources estimated in the Nold group and the abnormal increase only in the ADD group. Specifically, the interhemispheric LLC solutions in the occipital delta sources were higher in the ADD than the Nold and PDD groups. Furthermore, the intrahemispheric LLC solutions in distributed delta sources were greater in the ADD than the Nold group, whereas those LLC solutions in temporal delta sources were higher in the ADD than the Nold, PDD, and DLB groups.

The fact that delta source connectivity was abnormal in the ADD group but not in the DLB and PDD groups was surprising as the delta sources of rsEEG rhythms were more abnormal in the same DLB and PDD patients compared with the AD ones in our previous reference study (Babiloni et al., 2017). We discussed this surprising dissociation of delta source "synchronization/desynchronization" and "functional cortical connectivity" in a subsequent paragraph.

The present findings agree with a previous study comparing LLC solutions in delta sources between Nold and ADD individuals (Babiloni et al., 2016a). Furthermore, they enrich with spatial details and individual frequency bands previous evidence showing differences in functional connectivity measurements from delta rhythms at scalp sensors between Nold and ADD individuals (Adler et al., 2003; Blinowska et al., 2017; Knott et al., 2000; Locatelli et al., 1998; Sankari et al., 2011).

The present evidence of normal delta LLC solutions in DLB and PDD patients contrasts previous findings showing lower (Andersson et al., 2008; van Dellen et al., 2015) or higher (Kai et al., 2005; van Dellen et al., 2015) delta connectivity in DLB compared with ADD patients. At the present early stage of the research, we cannot give a final explanation for these discrepancies. It is unclear if they depend on (1) the current technique of multivariate LLC rather than bivariate coherence for the estimation of the rsEEG functional interdependence; (2) the computation of the functional connectivity at the cortical source rather than the scalp sensor level (e.g., LLC solutions in the source space and spectral coherence computed between scalp electrode pairs may be differently affected by residual ocular or muscular artifacts in the EEG signals); and (3) the use of individual rather than fixed frequency bands for the analysis of delta rhythms. Future studies should vary the mentioned methodological options systematically in the same database to clarify the matter.

The neurophysiological mechanism generating human delta rhythms in quiet wakefulness is poorly known. A speculative explanation is that normal delta rhythms in quiet wakefulness are generated by intrinsic thalamocortical interactions associated with a relative functional isolation of cortical modules from the sensory flow, analogously to the neurophysiological mechanism producing slow waves in non-REM sleep (Crunelli et al., 2015). Another speculative explanation is that the generating mechanism might be the "stand-by" mode of selective circuits of corticothalamic and relay thalamocortical neurons engaged in fast information processing during cognitive tasks (Taylor et al., 2014).

In the aforementioned theoretical framework, it can be just speculated that the present evidence of an abnormal posterior delta source connectivity in the ADD patients might reflect an abnormal upregulation of the mechanisms generating normal delta rhythms in quiet wakefulness. In ADD patients, that upregulation might result from cortical blood hypoperfusion and synaptic dysfunction in the same regions (Niedermeyer et al., 1997; Passero et al., 1995; Rodriguez et al., 1999; Valladares-Neto et al., 1995). Other causes might be a white matter lesion (Agosta et al., 2013, 2014) or the loss of neurons in the cortical gray matter, especially in the posterior cortex (Delli Pizzi et al., 2014, 2015, 2016; Babiloni et al., 2013, 2015; Fernandez et al., 2003; Graff-Radford et al., 2016; Sarro et al., 2016).

4.3. The LLC solutions in delta and alpha sources classified Nold participants versus patients with dementia

Here, we report the results of 2 exploratory analyses aimed at testing the clinically relevance of the present findings. The first analysis showed significant positive correlations between MMSE scores (roughly reflecting global cognitive status) and LLC solutions in interhemispheric temporal and intrahemispheric diffuse alpha sources across all Nold, ADD, DLB, and PDD individuals as a whole group. However, even if statistically significant ($p < 0.005$), the correlation values were relatively low as variance explained (i.e., $r = 0.24–0.26$). Furthermore, no statistically significant correlation ($p > 0.05$) was observed for any single group considered separately. The present findings suggest that neurophysiological mechanisms of the interdependence of cortical neural synchronization/desynchronization underpinning brain arousal and low vigilance (as reflected in the LLC solutions of this study) are only one of the determinants of global cognitive functions in human participants. Other relevant neurophysiological mechanisms

involved in cognitive information processes may be those related to selective attention, encoding and retrieval of information in long-term memory, frontal executive functions (some assisted by internal language), and others. Therefore, future studies may measure functional connectivity not only during the resting-state condition (i.e., low vigilance) but also during attention, episodic and working memory, and other cognitive tasks. The derived EEG markers may be used as a multivariate input for linear (logistics regression) and nonlinear (artificial neural networks or support vector machines) predictors of the MMSE score in Nold participants and patients with dementing disorders. The expected results may show high correlation values and remarkable insights about the derangement of brain functions in the evolution of dementing disorders.

The second analysis pointed to a moderate classification accuracy of several alpha LLC solutions in the discrimination of ADD versus Nold, DLB, and PDD individuals. Specifically, interhemispheric LLC solutions in the temporal alpha sources showed an AUROC curve of 0.84 versus Nold individuals and 0.75 versus DLB individuals, whereas intrahemispheric LLC solutions in the central alpha sources exhibited an AUROC curve of 0.78 versus PDD individuals. Noteworthy, the only substantial classification accuracy of the LLC solutions in delta sources was obtained with the interhemispheric LLC solutions in occipital delta sources discriminating Nold participants versus ADD patients (e.g., AUROC curve of 0.7).

The present findings are in line with previous evidence showing the following values of classification accuracy (1) 0.45–1.0 for Nold versus ADD individuals (e.g., 1 = 100%); (2) 0.78–0.92 for MCI versus ADD individuals; and (3) 0.60–0.87 for the conversion from MCI to ADD status (Adler et al., 2003; Babiloni et al., 2015, 2016b; Bennys et al., 2001; Blinowska et al., 2017; Brassen et al., 2004; Buscema et al., 2007; Claus et al., 1999; Engedal et al., 2015; Garn et al., 2017; Huang et al., 2000; Jelic et al., 2000; Knyazeva et al., 2010; Lehmann et al., 2007; Lizio et al., 2016; Missonnier et al., 2006; Nuwer, 1997).

Concerning the classification of Nold versus DLB and PDD individuals, the present discrimination with 0.75–0.78 of success was intermediate when compared with those reported in previous studies. In those investigations, global delta and alpha coherences between electrode pairs allowed a classification accuracy of 0.75–0.80 of DLB individuals compared with Nold participants (Andersson et al., 2008). Another study (Roks et al., 2008) used the grand total EEG score to discriminate DLB versus Nold individuals with an accuracy of 0.78. Finally, 2 advanced procedures using a combination of 20–25 discriminant rsEEG power density and connectivity measurements showed a classification accuracy of 0.80–1.0 between PDD/DLB and Nold individuals (Engedal et al., 2015; Garn et al., 2017; Snaedal et al., 2012). Noteworthy, no previous cross-validated comparisons showed the ability of rsEEG markers in the discrimination of PDD versus DLB patients to delineate the bounds between these entities at the individual level.

4.4. The clinical neurophysiological model

In the reference study carried out in the same populations of the present investigation (Babiloni et al., 2017), rsEEG markers of "synchronization/desynchronization" were investigated. Results of that previous study suggest that posterior alpha source synchronization reduced dramatically in the ADD group, markedly in the DLB group, and moderately in the PDD group. In contrast, posterior delta source synchronization increased dramatically in the PDD group, markedly in the DLB group, and moderately in the ADD group. Compared to those findings, the present markers of "functional cortical connectivity" suggest maximum abnormalities of both delta and alpha source connectivity in the ADD group compared with the DLB and PDD groups, thus confirming the working hypothesis of this study. Interestingly, the present markers of "functional cortical connectivity" also suggest more abnormalities of alpha source connectivity in the DLB group compared with the PDD group.

Keeping in mind these findings, 2 main considerations can be done. The first consideration is that the markers of the neurophysiological reserve lead support to the concept of ADD as "cortical disconnection syndrome." The second consideration is that the combination of the markers of "synchronization/desynchronization" and "functional cortical connectivity" might enrich the assessment of cholinergic and dopaminergic neurotransmission in ADD, DLB, and PDD.

Based on the present results and those of Babiloni et al. (2017), the distinguishing markers of the neurophysiological reserve in ADD patients might be a dramatic decrease of both "synchronization/desynchronization" and "functional cortical connectivity" in posterior alpha sources. Furthermore, these patients might show an increase of both those markers in posterior delta sources.

In contrast, the distinguishing markers of the neurophysiological reserve in PDD and DLB patients might be a dissociation of "synchronization/desynchronization" and "functional cortical connectivity" markers in posterior delta sources, namely a marked increase of the former without a related increase of the latter.

In this framework, ADD patients exhibited more similarities to DLB than PDD patients for both markers of "synchronization" and "functional cortical connectivity" in alpha and delta sources.

An exciting hypothesis for future studies is that those markers of the neurophysiological reserve might reflect cholinergic dysfunction in the ADD, cholinergic and dopaminergic dysfunction in DLB, and dopaminergic dysfunction in the PDD. Those studies should correlate the hypothesized rsEEG markers of cholinergic and/or dopaminergic dysfunction and relevant PET readouts of dopaminergic and cholinergic uptake in the brain. More questionable may be the acute use of scopolamine and risperidone in ADD, DLB, and PDD patients for the risk of clinical side effects. Overall, the evaluation of that clinical neurophysiological model is motivated by some encouraging previous evidence reported in the following paragraphs.

Previous studies have unveiled a relationship between resting-state delta and alpha rhythms and cholinergic neurotransmission in ADD patients. Indeed, it has been shown that AChEI drugs (i.e., enhancing the cholinergic tone) exerted beneficial effects on some rsEEG frequency bands, namely decreasing delta (Adler and Brassen, 2001; Balkan et al., 2003; Gianotti et al., 2008; Reeves et al., 2002) and theta (Adler et al., 2004; Brassen and Adler, 2003; Gianotti et al., 2008) and increasing alpha power density (Agnoli et al., 1983; Babiloni et al., 2006c; Balkan et al., 2003).

In healthy participants, an acute dose of scopolamine (i.e., a muscarinic cholinergic antagonist) compared with placebo transiently increased delta and theta power density while reduced alpha and beta power density, in the way typically found in ADD patients (Ebert and Kirch, 1998). In addition, the scopolamine increased delta and reduced alpha power density in relation to plasma drug concentration and transient psychomotor impairment (Liem-Moolenaar et al., 2011a).

In both Nold and ADD patients, the acute scopolamine intervention induced decreased alpha power density and increased delta power density, the drop in the Nold participants being stronger as expected by the integrity of their cholinergic neurotransmission (Neufeld et al., 1994). More recently, an acute dose of scopolamine produced deranging effects on composite measurements of power density and coherence of delta, theta, alpha, beta, and gamma that had been successfully used to classify Nold and ADD individuals (Johannsson et al., 2015; Snaedal et al., 2010).

Unfortunately, less clear is the relationship between the mentioned rsEEG markers in delta sources and dopaminergic neurotransmission in PDD and DLB patients. Some previous studies provided support to the hypothesized relationship. Compared with Nold participants, PD patients showed higher delta and theta power density in several scalp regions, more evident in association with a progressive cognitive impairment (Bonanni et al., 2008; Caviness et al., 2007; Morita et al., 2009, 2011; Pugnetti et al., 2010). Furthermore, these features appeared to be specific, as delta and theta power density values were higher in PDD patients than in ADD, PD, and Nold participants (Babiloni et al., 2011; Fonseca et al., 2013). Moreover, these features were specifically related to phosphorylation of α-synuclein in the posterior cingulate cortex (hub of the default mode network), namely the higher the α-synuclein load, the higher the global delta, the lower the global alpha power density, and the lower the frequency alpha peak (Caviness et al., 2016).

In the same line, global delta and theta power density and variability were higher in DLB than ADD patients (Andersson et al., 2008; Kai et al., 2005). The global delta power density fluctuated more in DLB than ADD patients within 1 hour of rsEEG recording (Andersson et al., 2008; Walker et al., 2000a,b).

In healthy participants, an acute dose of risperidone (i.e., an atypical antipsychotic dopamine and serotonergic antagonist) compared with placebo transiently increased delta and/or theta power density of rsEEG rhythms in relation to plasma drug concentration (Lee et al., 1999) and transient psychomotor impairment (Hughes et al., 1999; Liem-Moolenaar et al., 2011b).

Noteworthy, other studies challenge the specificity of the relationship between the mentioned rsEEG markers in delta sources and dopaminergic neurotransmission in PDD and DLB patients. It was reported that treatment with AChEI (i.e., donepezil) partially normalized delta and theta power density (but not alpha) in DLB patients, whereas there was no significant difference in ADD patients. (Kai et al., 2005). Furthermore, L-dopa and electrical stimulation of subthalamic nucleus enhancing the dopaminergic tone reduced intrahemispheric frontoparietal alpha and beta (but not delta) coherences in association with an improvement of motor symptoms in PD patients (Moazami-Goudarzi et al., 2008; Silberstein et al., 2005). Also, intrahemispheric fronto-temporo-central delta and theta coherences were higher in DLB than in ADD patients (Andersson et al., 2008). Finally, global alpha coherence over the whole scalp was lower in DLB than ADD patients while global delta coherence was higher in the former than in the latter group (Andersson et al., 2008).

These mixed results in the literature confirms the complexity of the interactions and confounds related to comorbidities (e.g., depression, behavioral symptoms), psychoactive drugs, different stages of the diseases, and different levels of the impairment in cholinergic and dopaminergic systems in ADD, DLB, and PDD patients. A possible design to disentangle these variables may be a longitudinal study in de novo ADD, DLB, and PDD patients, free from major depression, to be undergone to rsEEG recordings before and after chronic administration of cholinergic and dopaminergic therapy. In these patients, levels of the impairment in cholinergic and dopaminergic systems may be measured by PET using radio ligands for cholinergic markers and DaTscan, respectively. Of note, those radio ligands for cholinergic markers such as [^{11}C]MP4A and [^{11}C]PMP PET for acetylcholinesterase, [^{123}I]5IA SPECT for the $\alpha_4\beta_2$ nicotinic acetylcholine receptor, and [^{123}I]IBVM SPECT for the vesicular acetylcholine transporter have shown that cortical acetylcholinesterase was reduced in PDD and ADD patients in relation with the level of performance in attention and working memory tests (see a review in Roy et al., 2016).

4.5. Methodological remarks

In the reference study carried out in the same populations (Babiloni et al., 2017), we discussed some methodological limitations of this retrospective and explorative study. Summarizing, these limitations include the relatively small number of the patients (N = 34–42) and the lack of (1) unified experimental recording protocol, (2) harmonized hardware for EEG recordings and neuroimaging, (3) extensive neuroimaging (e.g., DaTscan), (4) neuropsychological battery (e.g., Alzheimer's Disease Assessment Scale-cognitive subscale) in all clinical units (e.g., the MMSE score may be not equally sensitive to global cognitive deficits in all neurodegenerative dementing disorders), (5) groups of patients with prodromal stages of the disease (i.e., no antidementia pharmacological therapy), and (6) repeated recordings over time.

Here, 2 additional methodological limitations are discussed. In the present study, 128-Hz sampling rate was used for the data analysis as a frequency available in all clinical units of this international consortium. Noteworthy, this sampling rate is not optimal for the analysis of gamma band, especially for frequencies higher than 40 Hz. An optimal setting of EEG recording parameters may use 256 or 512 Hz to cover the whole gamma range and high-frequency oscillations >40 Hz. However, the use of 128-Hz sampling rate did not affect the main findings of the present study found at delta and alpha frequency bands, ranging <13 Hz. Furthermore, Figs. 2 and 3 of this article showed that the LLC solutions at beta 2 and gamma (20–40 Hz) bands were negligible in the present experimental conditions (i.e., eyes-closed resting state). Therefore, it is not probable that relevant effects may be observed at higher frequencies in these conditions.

In this study, another specific methodological limitation should be remarked. We used the toolbox LLC of eLORETA freeware (Pascual-Marqui et al., 2011) to estimate the functional connectivity between rsEEG cortical sources in Nold, ADD, PDD, and DLB groups of participants. Specifically, LLC estimates and removes zero-lag phase source interactions from the total linear connectivity in pairs of EEG cortical sources to mitigate at least in part the effects of head volume conduction (Pascual-Marqui et al., 2011). As a bivariate measurement of lagged interactions between 2 cortical sources, LLC may not remove the "common drive" effect of a third brain source sending action potentials to that pair of sources examined. This effect may cause a number of "false" connections between pairs of scalp sensors or source solutions in the readouts of the procedures (especially bivariate) used for estimation of EEG functional connectivity. Typically, those "false" connections are characterized by a "random" spatial topology. For this reason, we performed 4 control analyses to test the hypotheses that the present LLC solutions did not show a "random" spatial scheme between the pairs of ROIs in the Nold and the dementia groups. As an example, we used the LLC solutions computed for alpha rhythms. Results of these control analyses were not in line with a "random" topology of the pattern of functional EEG source connectivity of alpha rhythms (as reference dominant rsEEG rhythms) in the Nold group. In the same vein, they did not show a "random" topology of the pattern of the differences in functional EEG source connectivity of alpha rhythms between the Nold and the dementia groups. However, the present results did not exclude that part of the shown effects were due to common drive phenomenon. Therefore, future investigations will have to address this issue on simulated and real data, allowing a better understanding of the reliability and validity of the LLC estimates of rsEEG source connectivity with reference to head volume conduction and common drive/source effects. In this line, other EEG functional connectivity metrics, which are related to Granger causality, may be helpful to exclude the spurious lagged connectivity due to head volume conduction and common drive

effects. These are the directed transfer function (Kamiński and Blinowska, 1991) and the partial directed coherence (Baccalá and Sameshima, 2001). In the original implementations, both procedures are grounded on phase differences between EEG signals recorded at scalp electrodes. Among them, directed transfer function shows not only direct but also cascade flows, namely in case of propagation when there is a phase difference between signals (Blinowska, 2011). Another interesting procedure is the computation of "isolated effective coherence", estimating the partial coherence in the eLORETA source space under a multivariate autoregressive model (Pascual-Marqui et al., 2014).

5. Conclusions

Previous evidence showed abnormal markers of cortical neural "synchronization/desynchronization" in quiet wakefulness in ADD, DLB, and PDD patients, as revealed by posterior sources of delta (<4 Hz) and alpha (8–12 Hz) rhythms (Babiloni et al., 2017). We proposed that those markers might probe the neurophysiological reserve in those patients. The present exploratory study tested the hypothesis that another class of markers might probe the patients' neurophysiological reserve, namely the markers of "functional cortical connectivity." These markers might be especially informative in AD individuals, supposed to suffer from a "disconnection cortical syndrome" (Bokde et al., 2009; Teipel et al., 2016).

At the group level, the present results indicated that interhemispheric and intrahemispheric LLC solutions in widespread delta sources were abnormally higher in the ADD group and, surprisingly, normal in the DLB and PDD groups. Intrahemispheric LLC solutions were reduced in widespread alpha sources dramatically in the ADD group, markedly in the DLB group, and moderately in the PDD group. Furthermore, the interhemispheric LLC solutions showed lower values in the ADD and DLB groups than the PDD group.

At the individual level, AUROC curves of LLC solutions in alpha sources exhibited better classification accuracies for the discrimination of ADD versus Nold individuals (0.84) than for Nold versus DLB (0.78) and Nold versus PDD alpha (0.75).

These findings suggest that functional cortical connectivity in both delta and alpha sources might unveil a more compromised neurophysiological reserve in ADD than DLB, at both group and individual levels. This effect might occur interhemispherically and intrahemispherically, with more discrimination between the ADD and DLB groups interhemispherically.

These findings motivate future prospective, multicenter studies using a detailed evaluation of the patients' cognitive status, harmonized EEG hardware systems, and unique data collection protocols. Those future studies will aim to cross-validate the present results and improve our understanding of the effects of neurodegenerative dementing disorders on the rsEEG markers of the neurophysiological reserve, namely those of "synchronization/desynchronization" and "functional cortical connectivity." An exciting hypothesis for those studies is that the combination of "synchronization/desynchronization" and "functional cortical connectivity" markers might be valid topographic biomarkers of ADD, DLB, and PDD for clinical applications and research (i.e., the stratification of patients based on an index of neurophysiological reserve and the evaluation over time of the mechanistic effect of interventions).

Disclosure statement

The authors have no actual or potential conflicts of interest.

Acknowledgements

The present study was developed based on the data of the informal European Consortium PDWAVES and European Consortium of Dementia with Lewy Body. The members and institutional affiliations of the consortia are reported in the cover page of this manuscript. The research activities of the Unit of University of Rome "La Sapienza" were partially supported by the H2020 Marie S. Curie ITN-ETN project with the short title "BBDiag" (http://bbdiag-itn-etn.eu). We thank Mrs. Jessica Janson and Mrs. Marina Selivanova for their support to those activities in the framework of the BBDiag project.

Appendix A. Supplementary data

Supplementary data associated with this article can be found, in the online version, at https://doi.org/10.1016/j.neurobiolaging.2017.12.023.

References

Aarsland, D., Litvan, I., Salmon, D., Galasko, D., Wentzel-Larsen, T., Larsen, J.P., 2003. Performance on the dementia rating scale in Parkinson's disease with dementia and dementia with Lewy bodies: comparison with progressive supranuclear palsy and Alzheimer's disease. J. Neurol. Neurosurg. Psychiatry 74, 1215–1220.

Abdelnour, C., van Steenoven, I., Londos, E., Blanc, F., Auestad, B., Kramberger, M.G., Zetterberg, H., Mollenhauer, B., Boada, M., Aarsland, D. European DLB Consortium, 2016. Alzheimer's disease cerebrospinal fluid biomarkers predict cognitive decline in Lewy body dementia. Mov. Disord. 31, 1203–1208.

Adler, G., Brassen, S., 2001. Short-term rivastigmine treatment reduces EEG slow-wave power in Alzheimer patients. Neuropsychobiology 43, 273–276.

Adler, G., Brassen, S., Chwalek, K., Dieter, B., Teufel, M., 2004. Prediction of treatment response to rivastigmine in Alzheimer's dementia. J. Neurol. Neurosurg. Psychiatry 75, 292–294.

Adler, G., Brassen, S., Jajcevic, J., 2003. EEG coherence in Alzheimer's dementia. J. Neural Transm. 110, 1051–1058.

Agnoli, A., Martucci, N., Manna, V., Conti, L., Fioravanti, M., 1983. Effect of cholinergic and anticholinergic drugs on short-term memory in Alzheimer's dementia: a neuropsychological and computerized electroencephalographic study. Clin. Neuropharmacol. 6, 311–323.

Agosta, F., Canu, E., Stefanova, E., Sarro, L., Tomić, A., Špica, V., Comi, G., Kostić, V.S., Filippi, M., 2014. Mild cognitive impairment in Parkinson's disease is associated with a distributed pattern of brain white matter damage. Hum. Brain Mapp. 35, 1921–1929.

Agosta, F., Canu, E., Stojković, T., Pievani, M., Tomić, A., Sarro, L., Dragašević, N., Copetti, M., Comi, G., Kostić, V.S., Filippi, M., 2013. The topography of brain damage at different stages of Parkinson's disease. Hum. Brain Mapp. 34, 2798–2807.

Albert, M.S., DeKosky, S.T., Dickson, D., Dubois, B., Feldman, H.H., Fox, N.C., Gamst, A., Holtzman, D.M., Jagust, W.J., Petersen, R.C., Snyder, P.J., Carrillo, M.C., Thies, B., Phelps, C.H., 2011. The diagnosis of mild cognitive impairment due to Alzheimer's disease: recommendations from the National Institute on Aging-Alzheimer's Association workgroups on diagnostic guidelines for Alzheimer's disease. Alzheimers Dement. 7, 270–279.

American Academy of Sleep Medicine, 2014. International Classification of Sleep Disorders, Third Ed. American Academy of Sleep Medicine, Darien, IL.

American Psychiatric Association, 2000. Diagnostic and Statistical Manual of Mental Disorders (4th ed., Rev). Washington DC.

Andersson, M., Hansson, O., Minthon, L., Rosén, I., Londos, E., 2008. Electroencephalogram variability in dementia with Lewy bodies, Alzheimer's disease and controls. Dement. Geriatr. Cogn. Disord. 26, 284–290.

Anghinah, R., Kanda, P.A., Jorge, M.S., Lima, E.E., Pascuzzi, L., Melo, A.C., 2000. Alpha band coherence analysis of EEG in healthy adult's and Alzheimer's type dementia patients. Arq. Neuropsiquiatr. 58, 272–275.

Anonymous, 1994. Clinical and neuropathological criteria for fontotemporal dementia. The Lund and Manchester Groups. J. Neurol. Neurosurg. Psychiatry 57, 416–418.

Babiloni, C., Binetti, G., Cassetta, E., Dal Forno, G., Del Percio, C., Ferreri, F., Ferri, R., Frisoni, G., Hirata, K., Lanuzza, B., Miniussi, C., Moretti, D.V., Nobili, F., Rodriguez, G., Romani, G.L., Salinari, S., Rossini, P.M., 2006a. Sources of cortical rhythms change as a function of cognitive impairment in pathological aging: a multi-centric study. Clin. Neurophysiol. 117, 252–268.

Babiloni, C., Carducci, F., Lizio, R., Vecchio, F., Baglieri, A., Bernardini, S., Cavedo, E., Bozzao, A., Buttinelli, C., Esposito, F., Giubilei, F., Guizzaro, A., Marino, S., Montella, P., Quattrocchi, C.C., Redolfi, A., Soricelli, A., Tedeschi, G., Ferri, R., Rossi-Fedele, G., Ursini, F., Scrascia, F., Vernieri, F., Pedersen, T.J., Hardemark, H.G., Rossini, P.M., Frisoni, G.B., 2013. Resting state cortical electroencephalographic rhythms are related to gray matter volume in subjects

with mild cognitive impairment and Alzheimer's disease. Hum. Brain Mapp. 34, 1427–1446.
Babiloni, C., Cassetta, E., Dal Forno, G., Del Percio, C., Ferreri, F., Ferri, R., Lanuzza, B., Miniussi, C., Moretti, D.V., Nobili, F., Pascual-Marqui, R.D., Rodriguez, G., Luca Romani, G., Salinari, S., Zanetti, O., Rossini, P.M., 2006c. Donepezil effects on sources of cortical rhythms in mild Alzheimer's disease: Responders vs. Non-Responders. Neuroimage 31, 1650–1665.
Babiloni, C., De Pandis, M.F., Vecchio, F., Buffo, P., Sorpresi, F., Frisoni, G.B., Rossini, P.M., 2011. Cortical sources of resting state electroencephalographic rhythms in Parkinson's disease related dementia and Alzheimer's disease. Clin. Neurophysiol. 122, 2355–2364.
Babiloni, C., Del Percio, C., Boccardi, M., Lizio, R., Lopez, S., Carducci, F., Marzano, N., Soricelli, A., Ferri, R., Triggiani, A.I., Prestia, A., Salinari, S., Rasser, P.E., Basar, E., Famà, F., Nobili, F., Yener, G., Emek-Savaş, D.D., Gesualdo, L., Mundi, C., Thompson, P.M., Rossini, P.M., Frisoni, G.B., 2015. Occipital sources of resting-state alpha rhythms are related to local gray matter density in subjects with amnesic mild cognitive impairment and Alzheimer's disease. Neurobiol. Aging 36, 556–570.
Babiloni, C., Del Percio, C., Lizio, R., Noce, G., Cordone, S., Lopez, S., Soricelli, A., Ferri, R., Pascarelli, M.T., Nobili, F., Arnaldi, D., Aarsland, D., Orzi, F., Buttinelli, C., Giubilei, F., Onofrj, M., Stocchi, F., Stirpe, P., Fuhr, P., Gschwandtner, U., Ransmayr, G., Caravias, G., Garn, H., Sorpresi, F., Pievani, M., Frisoni, G.B., D'Antonio, F., De Lena, C., Güntekin, B., Hanoğlu, L., Başar, E., Yener, G., Emek-Savaş, D.D., Triggiani, A.I., Franciotti, R., De Pandis, M.F., Bonanni, L., 2017. Abnormalities of cortical neural synchronization mechanisms in patients with dementia due to Alzheimer's and Lewy body diseases: an EEG study. Neurobiol. Aging 55, 143–158.
Babiloni, C., Ferri, R., Binetti, G., Cassarino, A., Dal Forno, G., Ercolani, M., Ferreri, F., Frisoni, G.B., Lanuzza, B., Miniussi, C., Nobili, F., Rodriguez, G., Rundo, F., Stam, C.J., Musha, T., Vecchio, F., Rossini, P.M., 2006b. Fronto-parietal coupling of brain rhythms in mild cognitive impairment: a multicentric EEG study. Brain Res. Bull. 69, 63–73.
Babiloni, C., Ferri, R., Moretti, D.V., Strambi, A., Binetti, G., Dal Forno, G., Ferreri, F., Lanuzza, B., Bonato, C., Nobili, F., Rodriguez, G., Salinari, S., Passero, S., Rocchi, R., Stam, C.J., Rossini, P.M., 2004. Abnormal fronto-parietal coupling of brain rhythms in mild Alzheimer's disease: a multicentric EEG study. Eur. J. Neurosci. 19, 2583–2590.
Babiloni, C., Frisoni, G.B., Vecchio, F., Pievani, M., Geroldi, C., De Carli, C., Ferri, R., Vernieri, F., Lizio, R., Rossini, P.M., 2010. Global functional coupling of resting EEG rhythms is related to white-matter lesions along the cholinergic tracts in subjects with amnesic mild cognitive impairment. J. Alzheimer's Dis. 19, 859–871.
Babiloni, C., Lizio, R., Marzano, N., Capotosto, P., Soricelli, A., Triggiani, A.I., Cordone, S., Gesualdo, L., Del Percio, C., 2016a. Brain neural synchronization and functional coupling in Alzheimer's disease as revealed by resting state EEG rhythms. Int. J. Psychophysiol. 103, 88–102.
Babiloni, C., Triggiani, A.I., Lizio, R., Cordone, S., Tattoli, G., Bevilacqua, V., Soricelli, A., Ferri, R., Nobili, F., Gesualdo, L., Millán-Calenti, J.C., Buján, A., Tortelli, R., Cardinali, V., Barulli, M.R., Giannini, A., Spagnolo, P., Armenise, S., Buenza, G., Scianatico, G., Logroscino, G., Frisoni, G.B., Del Percio, C., 2016b. Classification of single normal and Alzheimer's disease individuals from cortical sources of resting state EEG rhythms. Front. Neurosci. 10, 47.
Baccalá, L.A., Sameshima, K., 2001. Partial directed coherence: a new concept in neural structure determination. Biol. Cybern. 84, 463–474.
Balkan, S., Yaraş, N., Mihçi, E., Dora, B., Ağar, A., Yargiçoğlu, P., 2003. Effect of donepezil on EEG spectral analysis in Alzheimer's disease. Acta Neurol. Belg. 103, 164–169.
Ballard, C., Grace, J., McKeith, I., Holmes, C., 1998. Neuroleptic sensitivity in dementia with Lewy bodies and Alzheimer's disease. Lancet 351, 1032–1033.
Barker, R.A., Williams-Gray, C.H., 2016. Review: the spectrum of clinical features seen with alpha synuclein pathology. Neuropathol. Appl. Neurobiol. 42, 6–19.
Bennys, K., Rondouin, G., Vergnes, C., Touchon, J., 2001. Diagnostic value of quantitative EEG in Alzheimer disease. Neurophysiol. Clin. 31, 153–160.
Besthorn, C., Förstl, H., Geiger-Kabisch, C., Sattel, H., Gasser, T., Schreiter-Gasser, U., 1994. EEG coherence in Alzheimer disease. Electroencephalogr. Clin. Neurophysiol. 90, 242–245.
Bhat, S., Acharya, U.R., Dadmehr, N., Adeli, H., 2015. Clinical neurophysiological and automated EEG-based diagnosis of the Alzheimer's disease. Eur. Neurol. 74, 202–210.
Blinowska, K.J., 2011. Review of the methods of determination of directed connectivity from multichannel data. Med. Biol. Eng. Comput. 49, 521–529.
Blinowska, K.J., Rakowski, F., Kaminski, M., De Vico Fallani, F., Del Percio, C., Lizio, R., Babiloni, C., 2017. Functional and effective brain connectivity for discrimination between Alzheimer's patients and healthy individuals: a study on resting state EEG rhythms. Clin. Neurophysiol. 128, 667–680.
Bokde, A.L., Ewers, M., Hampel, H., 2009. Assessing neuronal networks: understanding Alzheimer's disease. Prog. Neurobiol. 89, 125–133.
Bonanni, L., Thomas, A., Tiraboschi, P., Perfetti, B., Varanese, S., Onofrj, M., 2008. EEG comparisons in early Alzheimer's disease, dementia with Lewy bodies and Parkinson's disease with dementia patients with a 2-year follow-up. Brain 131 (Pt 3), 690–705.
Bonanni, L., Perfetti, B., Bifolchetti, S., Taylor, J.P., Franciotti, R., Parnetti, L., Thomas, A., Onofrj, M., 2015. Quantitative electroencephalogram utility in predicting conversion of mild cognitive impairment to dementia with Lewy bodies. Neurobiol. Aging 36, 434–445.
Bonanni, L., Franciotti, R., Nobili, F., Kramberger, M.G., Taylor, J.P., Garcia-Ptacek, S., Falasca, N.W., Famá, F., Cromarty, R., Onofrj, M., Aarsland, D. E-DLB study group, 2016. EEG markers of dementia with Lewy bodies: a multicenter cohort study. J. Alzheimers Dis. 54, 1649–1657.
Bosboom, J.L., Stoffers, D., Stam, C.J., van Dijk, B.W., Verbunt, J., Berendse, H.W., Wolters, ECh, 2006. Resting state oscillatory brain dynamics in Parkinson's disease: an MEG study. Clin. Neurophysiol. 117, 2521–2531.
Bosboom, J.L., Stoffers, D., Wolters, ECh, Stam, C.J., Berendse, H.W., 2009. MEG resting state functional connectivity in Parkinson's disease related dementia. J. Neural Transm. 116, 193–202.
Brassen, S., Adler, G., 2003. Short-term effects of acetylcholinesterase inhibitor treatment on EEG and memory performance in Alzheimer patients: an open, controlled trial. Pharmacopsychiatry 36, 304–308.
Brassen, S., Braus, D.F., Weber-Fahr, W., Tost, H., Moritz, S., Adler, G., 2004. Late-onset depression with mild cognitive deficits: electrophysiological evidences for a preclinical dementia syndrome. Dement. Geriatr. Cogn. Disord. 18, 271–277.
Breslau, J., Starr, A., Sicotte, N., Higa, J., Buchsbaum, M.S., 1989. Topographic EEG changes with normal aging and SDAT. Electroencephalogr. Clin. Neurophysiol. 72, 281–289.
Briel, R.C., McKeith, I.G., Barker, W.A., Hewitt, Y., Perry, R.H., Ince, P.G., Fairbairn, A.F., 1999. EEG findings in dementia with Lewy bodies and Alzheimer's disease. J. Neurol. Neurosurg. Psychiatry 66, 401–403.
Buscema, M., Rossini, P., Babiloni, C., Grossi, E., 2007. The IFAST model, a novel parallel nonlinear EEG analysis technique, distinguishes mild cognitive impairment and Alzheimer's disease patients with high degree of accuracy. Artif. Intell. Med. 40, 127–141.
Buter, T.C., van den, H.A., Matthews, F.E., Larsen, J.P., Brayne, C., Aarsland, D., 2008. Dementia and survival in Parkinson disease: a 12-year population study. Neurology 70, 1017–1022.
Caviness, J.N., Hentz, J.G., Evidente, V.G., Driver-Dunckley, E., Samanta, J., Mahant, P., Connor, D.J., Sabbagh, M.N., Shill, H.A., Adler, C.H., 2007. Both early and late cognitive dysfunction affects the electroencephalogram in Parkinson's disease. Parkinsonism Relat. Disord. 13, 348–354.
Caviness, J.N., Lue, L.F., Hentz, J.G., Schmitz, C.T., Adler, C.H., Shill, H.A., Sabbagh, M.N., Beach, T.G., Walker, D.G., 2016. Cortical phosphorylated α-Synuclein levels correlate with brain wave spectra in Parkinson's disease. Mov. Disord. 31, 1012–1019.
Claus, J.J., Strijers, R.L., Jonkman, E.J., Ongerboer de Visser, B.W., Jonker, C., Walstra, G.J., Scheltens, P., van Gool, W.A., 1999. The diagnostic value of electroencephalography in mild senile Alzheimer's disease. Clin. Neurophysiol. 110, 825–832.
Cummings, J.L., Mega, M., Gray, K., Rosenberg-Thompson, S., Carusi, D.A., Gornbein, J., 1994. The neuropsychiatric inventory: comprehensive assessment of psychopathology in dementia. Neurology 44, 2308–2314.
Crunelli, V., David, F., Lőrincz, M.L., Hughes, S.W., 2015. The thalamocortical network as a single slow wave-generating unit. Curr. Opin. Neurobiol. 31, 72–80.
D'Amelio, M., Rossini, P.M., 2012. Brain excitability and connectivity of neuronal assemblies in Alzheimer's disease: from animal models to human findings. Prog. Neurobiol. 99, 42–60.
Dauwan, M., van Dellen, E., van Boxtel, L., van Straaten, E.C., de Waal, H., Lemstra, A.W., Gouw, A.A., van der Flier, W.M., Scheltens, P., Sommer, I.E., Stam, C.J., 2016a. EEG-directed connectivity from posterior brain regions is decreased in dementia with Lewy bodies: a comparison with Alzheimer's disease and controls. Neurobiol. Aging 41, 122–129.
Dauwan, M., van der Zande, J.J., van Dellen, E., Sommer, I.E., Scheltens, P., Lemstra, A.W., Stam, C.J., 2016b. Random forest to differentiate dementia with Lewy bodies from Alzheimer's disease. Alzheimers Dement. (Amst) 4, 99–106.
DeLong, E.R., DeLong, D.M., Clarke-Pearson, D.L., 1988. Comparing the areas under two or more correlated receiver operating characteristic curves: a nonparametric approach. Biometrics 44, 837–845.
Dierks, T., Ihl, R., Frolich, L., Maurer, K., 1993. Dementia of the Alzheimer type: effects on the spontaneous EEG described by dipole sources. Psychiatry Res. 50, 151–162.
Dierks, T., Jelic, V., Pascual-Marqui, R.D., Wahlund, L.O., Julin, P., Linden, D.E.J., Maurer, K., Winblad, B., Nordberg, A., 2000. Spatial pattern of cerebral glucose metabolism (PET) correlates with localization of intracerebral EEG-generators in Alzheimer's disease. Clin. Neurophysiol. 111, 1817–1824.
Dubois, B., Feldman, H.H., Jacova, C., Hampel, H., Molinuevo, J.L., Blennow, K., DeKosky, S.T., Gauthier, S., Selkoe, D., Bateman, R., Cappa, S., Crutch, S., Engelborghs, S., Frisoni, G.B., Fox, N.C., Galasko, D., Habert, M.O., Jicha, G.A., Nordberg, A., Pasquier, F., Rabinovici, G., Robert, P., Rowe, C., Salloway, S., Sarazin, M., Epelbaum, S., de Souza, L.C., Vellas, B., Visser, P.J., Schneider, L., Stern, Y., Scheltens, P., Cummings, J.L., 2014. Advancing research diagnostic criteria for Alzheimer's disease: the IWG-2 criteria. Lancet Neurol. 13, 614–629.
Dubois, B., Pillon, B., 1997. Cognitive deficits in Parkinson's disease. J. Neurol. 244, 2–8. Review.
Dubois, B., Slachevsky, A., Litvan, I., Pillon, B., 2000. The FAB: a frontal assessment battery at bedside. Neurology 55, 1621–1626.
Delli Pizzi, S., Franciotti, R., Tartaro, A., Caulo, M., Thomas, A., Onofrj, M., Bonanni, L., 2014. Structural alteration of the dorsal visual network in DLB patients with visual hallucinations: a cortical thickness MRI study. PLoS One 9, e86624.
Delli Pizzi, S., Franciotti, R., Bubbico, G., Thomas, A., Onofrj, M., Bonanni, L., 2016. Atrophy of hippocampal subfields and adjacent extrahippocampal structures in dementia with Lewy bodies and Alzheimer's disease. Neurobiol. Aging 40, 103–109.

Delli Pizzi, S., Franciotti, R., Taylor, J.P., Esposito, R., Tartaro, A., Thomas, A., Onofrj, M., Bonanni, L., 2015. Structural connectivity is differently altered in dementia with Lewy body and Alzheimer's disease. Front. Aging Neurosci. 7, 208.
Dunkin, J.J., Leuchter, A.F., Newton, T.F., Cook, I.A., 1994. Reduced EEG coherence in dementia: state or trait marker? Biol. Psychiatry 35, 870–879.
Dunkin, J.J., Osato, S., Leuchter, A.F., 1995. Relationships between EEG coherence and neuropsychological tests in dementia. Clin. Electroencephalogr. 26, 47–59.
Ebert, U., Kirch, W., 1998. Scopolamine model of dementia: electroencephalogram findings and cognitive performance. Eur. J. Clin. Invest. 28, 944–949. Review.
Emre, M., Aarsland, D., Brown, R., Burn, D.J., Duyckaerts, C., Mizuno, Y., Broe, G.A., Cummings, J., Dickson, D.W., Gauthier, S., Goldman, J., Goetz, C., Korczyn, A., Lees, A., Levy, R., Litvan, I., McKeith, I., Olanow, W., Poewe, W., Quinn, N., Sampaio, C., Tolosa, E., Dubois, B., 2007. Clinical diagnostic criteria for dementia associated with Parkinson's disease. Mov. Disord. 22, 1689–1707.
Engedal, K., Snaedal, J., Hoegh, P., Jelic, V., Bo Andersen, B., Naik, M., Wahlund, L.O., Oeksengaard, A.R., 2015. Quantitative EEG applying the statistical recognition pattern method: a useful tool in dementia diagnostic workup. Dement. Geriatr. Cogn. Disord. 40, 1–12.
Fahn, S., Elton, R. Members of the UPDRS Development Committee, 1987. Unified Parkinson's disease rating scale. In: Fahn, S., Marsden, C.D., Calne, D.B., Goldstein, M. (Eds.), Recent Developments in Parkinson's Disease, Vol. 2. Macmillan Health Care Information, Florham Park, NJ, pp. 293–304.
Fernandez, A., Arrazola, J., Maestu, F., Amo, C., Gil-Gregorio, P., Wienbruch, C., Ortiz, T., 2003. Correlations of hippocampal atrophy and focal low-frequency magnetic activity in Alzheimer disease: volumetric MR imaging-magnetoencephalographic study. AJNR Am. J. Neuroradiol. 24, 481–487.
Folstein, M.F., Folstein, S.E., McHugh, P.R., 1975. 'Mini Mental State': a practical method for grading the cognitive state of patients for clinician. J. Psychiatr. Res. 12, 189–198.
Fonseca, L.C., Tedrus, G.M., Carvas, P.N., Machado, E.C., 2013. Comparison of quantitative EEG between patients with Alzheimer's disease and those with Parkinson's disease dementia. Clin. Neurophysiol. 124, 1970–1974.
Fonseca, L.C., Tedrus, G.M., Prandi, L.R., Almeida, A.M., Furlanetto, D.S., 2011. Alzheimer's disease: relationship between cognitive aspects and power and coherence EEG measures. Arq. Neuropsiquiatr. 69, 875–881.
Fünfgeld, E.W., 1995. Computerised brain electrical activity findings of Parkinson patients suffering from hyperkinetic side effects (hypersensitive dopamine syndrome) and a review of possible sources. J. Neural. Transm. Suppl. 46, 351–365.
Garn, H., Coronel, C., Waser, M., Caravias, G., Ransmayr, G., 2017. Differential diagnosis between patients with probable Alzheimer's disease, Parkinson's disease dementia, or dementia with Lewy bodies and frontotemporal dementia, behavioral variant, using quantitative electroencephalographic features. J. Neural Transm. (Vienna) 124, 569–581.
Gelb, D.J., Oliver, E., Gilman, S., 1999. Diagnostic criteria for Parkinson disease. Arch. Neurol. 56, 33–39.
Giaquinto, S., Nolfe, G., 1986. The EEG in the normal elderly: a contribution to the interpretation of aging and dementia. Electroencephalogr. Clin. Neurophysiol. 63, 540–546.
Gianotti, L.R., Künig, G., Faber, P.L., Lehmann, D., Pascual-Marqui, R.D., Kochi, K., Schreiter-Gasser, U., 2008. Rivastigmine effects on EEG spectra and three-dimensional LORETA functional imaging in Alzheimer's disease. Psychopharmacology (Berl) 198, 323–332.
Graff-Radford, J., Lesnick, T.G., Boeve, B.F., Przybelski, S.A., Jones, D.T., Senjem, M.L., Gunter, J.L., Ferman, T.J., Knopman, D.S., Murray, M.E., Dickson, D.W., Sarro, L., Jack Jr., C.R., Petersen, R.C., Kantarci, K., 2016. Predicting survival in dementia with Lewy bodies with hippocampal volumetry. Mov. Disord. 31, 989–994.
Hoehn, M.M., Yahr, M.D., 1967. Parkinsonism: onset, progression and mortality. Neurology 17, 427–442.
Huang, C., Wahlund, L.O., Dierks, T., Julin, P., Winblad, B., Jelic, V., 2000. Discrimination of Alzheimer's disease and mild cognitive impairment by equivalent EEG sources: a cross-sectional and longitudinal study. Clin. Neurophysiol. 11, 1961–1967.
Huber, S.J., Shuttleworth, E.C., Freidenberg, D.L., 1989. Neuropsychological differences between the dementias of Alzheimer's and Parkinson's diseases. Arch. Neurol. 46, 1287–1291.
Hughes, A.M., Lynch, P., Rhodes, J., Ervine, C.M., Yates, R.A., 1999. Electroencephalographic and psychomotor effects of chlorpromazine and risperidone relative to placebo in normal healthy volunteers. Br. J. Clin. Pharmacol. 48, 323–330.
Hughes, C.P., Berg, L., Danziger, W.L., Coben, L.A., Martin, R.L., 1982. A new clinical scale for the staging of dementia. Br. J. Psychiatry 140, 566–572.
Hughes, S.W., Crunelli, V., 2005. Thalamic mechanisms of EEG alpha rhythms and their pathological implications. Neuroscientist 11, 357–372.
Hughes, T.A., Ross, H.F., Musa, S., Bhattacherjee, S., Nathan, R.N., Mindham, R.H., Spokes, E.G., 2000. A 10-year study of the incidence of and factors predicting dementia in Parkinson's disease. Neurology 54, 1596–1602.
Irwin, D.J., Grossman, M., Weintraub, D., Hurtig, H.I., Duda, J.E., Xie, S.X., Lee, E.B., Van Deerlin, V.M., Lopez, O.L., Kofler, J.K., Nelson, P.T., Jicha, G.A., Woltjer, R., Quinn, J.F., Kaye, J., Leverenz, J.B., Tsuang, D., Longfellow, K., Yearout, D., Kukull, W., Keene, C.D., Montine, T.J., Zabetian, C.P., Trojanowski, J.Q., 2017. Neuropathological and genetic correlates of survival and dementia onset in synucleinopathies: a retrospective analysis. Lancet Neurol. 16, 55–65.
Jelic, V., Johansson, S.E., Almkvist, O., Shigeta, M., Julin, P., Nordberg, A., Winblad, B., Wahlund, L.O., 2000. Quantitative electroencephalography in mild cognitive impairment: longitudinal changes and possible prediction of Alzheimer's disease. Neurobiol. Aging 21, 533–540.
Jelic, V., Julin, P., Shigeta, M., Nordberg, A., Lannfelt, L., Winblad, B., Wahlund, L.O., 1997. Apolipoprotein E epsilon4 allele decreases functional connectivity in Alzheimer's disease as measured by EEG coherence. J. Neurol. Neurosurg. Psychiatry 63, 59–65.
Jeong, J., 2004. EEG dynamics in patients with Alzheimer's disease. Clin. Neurophysiol. 115, 1490–1505.
Johannsson, M., Snaedal, J., Johannesson, G.H., Gudmundsson, T.E., Johnsen, K., 2015. The acetylcholine index: an electroencephalographic marker of cholinergic activity in the living human brain applied to Alzheimer's disease and other dementias. Dement. Geriatr. Cogn. Disord. 39, 132–142.
Jurica, P.J., Leitten, C.L., Mattis, S., 2001. Dementia Rating Scale-2: Professional Manual. Psychological Assessment Resources, Lutz.
Kai, T., Asai, Y., Sakuma, K., Koeda, T., Nakashima, K., 2005. Quantitative electroencephalogram analysis in dementia with Lewy bodies and Alzheimer's disease. J. Neurol. Sci. 237, 89–95.
Kamei, S., Morita, A., Serizawa, K., Mizutani, T., Hirayanagi, K., 2010. Quantitative EEG analysis of executive dysfunction in Parkinson disease. J. Clin. Neurophysiol. 27, 193–197.
Kamiński, M.J., Blinowska, K.J., 1991. A new method of the description of the information flow in the brain structures. Biol. Cybern. 65, 203–210.
Karantzoulis, S., Galvin, J.E., 2013. Update on dementia with Lewy bodies. Curr. Transl. Geriatr. Exp. Gerontol. Rep. 2, 196–204.
Klimesch, W., 1996. Memory processes, brain oscillations and EEG synchronization. Int. J. Psychophysiol. 24, 61–100.
Klimesch, W., Doppelmayr, M., Russegger, H., Pachinger, T., Schwaiger, J., 1998. Induced alpha band power changes in the human EEG and attention. Neurosci. Lett. 244, 73–76.
Klimesch, W., 1999. EEG alpha and theta oscillations reflect cognitive and memory performance: a review and analysis. Brain Res. Rev. 29, 1169–1195.
Knott, V., Mohr, E., Mahoney, C., Ilivitsky, V., 2000. Electroencephalographic coherence in Alzheimer's disease: comparisons with a control group and population norms. J. Geriatr. Psychiatry Neurol. 13, 1–8.
Knyazeva, M.G., Jalili, M., Brioschi, A., Bourquin, I., Fornari, E., Hasler, M., Meuli, R., Maeder, P., Ghika, J., 2010. Topography of EEG multivariate phase synchronization in early Alzheimer's disease. Neurobiol. Aging 31, 1132–1144.
Kogan, E.A., Korczyn, A.D., Virchowsy, R.G., Klimovizky, SSh, Treves, T.A., Neufeld, M.Y., 2001. EEG changes during long-term treatment with donepezil in Alzheimer's disease patients. J. Neural. Transm. 108, 1167–1173.
Lawton, M.P., Brodie, E.M., 1969. Assessment of older people: self maintaining and instrumental activity of daily living. J. Gerontol. 9, 179–186.
Lee, D.Y., Lee, K.U., Kwon, J.S., Jang, I.J., Cho, M.J., Shin, S.G., Woo, J.I., 1999. Pharmacokinetic-pharmacodynamic modeling of risperidone effects on electroencephalography in healthy volunteers. Psychopharmacology (Berl) 144, 272–278.
Lehmann, C., Koenig, T., Jelic, V., Prichep, L., John, R.E., Wahlund, L.O., Dodge, Y., Dierks, T., 2007. Application and comparison of classification algorithms for recognition of Alzheimer's disease in electrical brain activity (EEG). J. Neurosci. Methods 161, 342–350.
Leuchter, A.F., Spar, J.E., Walter, D.O., Weiner, H., 1987. Electroencephalographic spectra and coherence in the diagnosis of Alzheimer's-type and multi-infarct dementia. A pilot study. Arch. Gen. Psychiatry 44, 993–998.
Leuchter, A.F., Dunkin, J.J., Lufkin, R.B., Anzai, Y., Cook, I.A., Newton, T.F., 1994. Effect of white matter disease on functional connections in the aging brain. J. Neurol. Neurosurg. Psychiatry 57, 1347–1354.
Leuchter, A.F., Newton, T.F., Cook, I.A., Walter, D.O., Rosenberg-Thompson, S., Lachenbruch, P.A., 1992. Changes in brain functional connectivity in Alzheimer-type and multi-infarct dementia. Brain 115 (Pt 5), 1543–1561.
Levy, A., Brandeis, R., Treves, T.A., Meshulam, Y., Mawassi, F., Feiler, D., Wengier, A., Glikfeld, P., Grunwald, J., Dachir, S., et al., 1994. Transdermal physostigmine in the treatment of Alzheimer's disease. Alzheimer Dis. Assoc. Disord. 81, 15–21.
Levy, G., Tang, M.X., Cote, L.J., Louis, E.D., Alfaro, B., Mejia, H., Stern, Y., Marder, K., 2000. Motor impairment in PD: relationship to incident dementia and age. Neurology 55, 539–544.
Liem-Moolenaar, M., de Boer, P., Timmers, M., Schoemaker, R.C., van Hasselt, J.G., Schmidt, S., van Gerven, J.M., 2011a. Pharmacokinetic-pharmacodynamic relationships of central nervous system effects of scopolamine in healthy subjects. Br. J. Clin. Pharmacol. 71, 886–898.
Liem-Moolenaar, M., Rad, M., Zamuner, S., Cohen, A.F., Lemme, F., Franson, K.L., van Gerven, J.M., Pich, E.M., 2011b. Central nervous system effects of the interaction between risperidone (single dose) and the 5-HT6 antagonist SB742457 (repeated doses) in healthy men. Br. J. Clin. Pharmacol. 71, 907–916.
Lizio, R., Del Percio, C., Marzano, N., Soricelli, A., Yener, G.G., Başar, E., Mundi, C., De Rosa, S., Triggiani, A.I., Ferri, R., Arnaldi, D., Nobili, F.M., Cordone, S., Lopez, S., Carducci, F., Santi, G., Gesualdo, L., Rossini, P.M., Cavedo, E., Mauri, M., Frisoni, G.B., Babiloni, C., 2016. Neurophysiological assessment of Alzheimer's disease individuals by a single electroencephalographic marker. J. Alzheimers Dis. 49, 159–177.
Locatelli, T., Cursi, M., Liberati, D., Franceschi, M., Comi, G., 1998. EEG coherence in Alzheimer's disease. Electroencephalogr. Clin. Neurophysiol. 106, 229–237.
Lörincz, M.L., Crunelli, V., Hughes, S.W., 2008. Cellular dynamics of cholinergically induced alpha (8-13 Hz) rhythms in sensory thalamic nuclei in vitro. J. Neurosci. 28, 660–671.

Lörincz, M.L., Kékesi, K.A., Juhász, G., Crunelli, V., Hughes, S.W., 2009. Temporal framing of thalamic relay-mode firing by phasic inhibition during the alpha rhythm. Neuron 63, 683–696.
McKeith, I.G., Boeve, B.F., Dickson, D.W., Halliday, G., Taylor, J.P., Weintraub, D., Aarsland, D., Galvin, J., Attems, J., Ballard, C.G., Bayston, A., Beach, T.G., Blanc, F., Bohnen, N., Bonanni, L., Bras, J., Brundin, P., Burn, D., Chen-Plotkin, A., Duda, J.E., El-Agnaf, O., Feldman, H., Ferman, T.J., Ffytche, D., Fujishiro, H., Galasko, D., Goldman, J.G., Gomperts, S.N., Graff-Radford, N.R., Honig, L.S., Iranzo, A., Kantarci, K., Kaufer, D., Kukull, W., Lee, V.M.Y., Leverenz, J.B., Lewis, S., Lippa, C., Lunde, A., Masellis, M., Masliah, E., McLean, P., Mollenhauer, B., Montine, T.J., Moreno, E., Mori, E., Murray, M., O'Brien, J.T., Orimo, S., Postuma, R.B., Ramaswamy, S., Ross, O.A., Salmon, D.P., Singleton, A., Taylor, A., Thomas, A., Tiraboschi, P., Toledo, J.B., Trojanowski, J.Q., Tsuang, D., Walker, Z., Yamada, M., Kosaka, K., 2017. Diagnosis and management of dementia with Lewy bodies: Fourth consensus report of the DLB Consortium. Neurology 89, 88–100.
McKeith, I.G., Dickson, D.W., Lowe, J., Emre, M., O'Brien, J.T., Feldman, H., Cummings, J., Duda, J.E., Lippa, C., Perry, E.K., Aarsland, D., Arai, H., Ballard, C.G., Boeve, B., Burn, D.J., Costa, D., Del Ser, T., Dubois, B., Galasko, D., Gauthier, S., Goetz, C.G., Gomez-Tortosa, E., Halliday, G., Hansen, L.A., Hardy, J., Iwatsubo, T., Kalaria, R.N., Kaufer, D., Kenny, R.A., Korczyn, A., Kosaka, K., Lee, V.M., Lees, A., Litvan, I., Londos, E., Lopez, O.L., Minoshima, S., Mizuno, Y., Molina, J.A., Mukaetova-Ladinska, E.B., Pasquier, F., Perry, R.H., Schulz, J.B., Trojanowski, J.Q., Yamada, M. Consortium on DLB, 2005. Diagnosis and management of dementia with Lewy bodies: third report of the DLB Consortium. Neurology 65, 1863–1872.
McKeith, I.G., Galasko, D., Kosaka, K., Perry, E.K., Dickson, D.W., Hansen, L.A., Salmon, D.P., Lowe, J., Mirra, S.S., Byrne, E.J., Lennox, G., Quinn, N.P., Edwardson, J.A., Ince, P.G., Bergeron, C., Burns, A., Miller, B.L., Lovestone, S., Collerton, D., Jansen, E.N., Ballard, C., de Vos, R.A., Wilcock, G.K., Jellinger, K.A., Perry, R.H., 1996. Consensus guidelines for the clinical and pathologic diagnosis of dementia with Lewy bodies (DLB): report of the consortium on DLB international workshop. Neurology 47, 1113–1124.
McKhann, G., Drachman, D., Folstein, M., Katzman, R., Price, D., Stadlan, E.M., 1984. Clinical diagnosis of Alzheimer's disease: report of the NINCDS-ADRDA Work Group under the auspices of Department of Health and Human Services Task Force on Alzheimer's disease. Neurology 34, 939–944.
McKhann, G.M., Knopman, D.S., Chertkow, H., Hyman, B.T., Jack Jr., C.R., Kawas, C.H., Klunk, W.E., Koroshetz, W.J., Manly, J.J., Mayeux, R., Mohs, R.C., Morris, J.C., Rossor, M.N., Scheltens, P., Carrillo, M.C., Thies, B., Weintraub, S., Phelps, C.H., 2011. The diagnosis of dementia due to Alzheimer's disease: recommendations from the National Institute on Aging-Alzheimer's Association workgroups on diagnostic guidelines for Alzheimer's disease. Alzheimers Dement. 7, 263–269.
Melgari, J.M., Curcio, G., Mastrolilli, F., Salomone, G., Trotta, L., Tombini, M., di Biase, L., Scrascia, F., Fini, R., Fabrizio, E., Rossini, P.M., Vernieri, F., 2014. Alpha and beta EEG power reflects L-dopa acute administration in parkinsonian patients. Front. Aging Neurosci. 6, 302.
Missonnier, P., Gold, G., Herrmann, F.R., Fazio-Costa, L., Michel, J.P., Deiber, M.P., Michon, A., Giannakopoulos, P., 2006. Decreased theta event-related synchronization during working memory activation is associated with progressive mild cognitive impairment. Dement. Geriatr. Cogn. Disord. 22, 250–259.
Moazami-Goudarzi, M., Sarnthein, J., Michels, L., Moukhtieva, R., Jeanmonod, D., 2008. Enhanced frontal low and high frequency power and synchronization in the resting EEG of parkinsonian patients. Neuroimage 41, 985–997.
Moretti, D.V., Babiloni, F., Carducci, F., Cincotti, F., Remondini, E., Rossini, P.M., Salinari, S., Babiloni, C., 2003. Computerized processing of EEG–EOG–EMG artifacts for multicentric studies in EEG oscillations and event-related potentials. Int. J. Pshycophysiol. 47, 199–216.
Morita, A., Kamei, S., Mizutani, T., 2011. Relationship between slowing of the EEG and cognitive impairment in Parkinson disease. J. Clin. Neurophysiol. 28, 384–387.
Morita, A., Kamei, S., Serizawa, K., Mizutani, T., 2009. The relationship between slowing EEGs and the progression of Parkinson's disease. J. Clin. Neurophysiol. 26, 426–429.
Neufeld, M.Y., Inzelberg, R., Korczyn, A.D., 1988. EEG in demented and non-demented parkinsonian patients. Acta Neurol. Scand. 78, 1–5.
Neufeld, M.Y., Rabey, M.J., Parmet, Y., Sifris, P., Treves, T.A., Korczyn, A.D., 1994. Effects of a single intravenous dose of scopolamine on the quantitative EEG in Alzheimer's disease patients and age-matched controls. Electroencephalogr. Clin. Neurophysiol. 91, 407–412.
Niedermeyer, E., Naidu, S.B., Plate, C., 1997. Unusual EEG theta rhythms over central region in Rett syndrome: considerations of the underlying dysfunction. Clin. Electroencephalogr. 28, 36–43.
Nuwer, M., 1997. Assessment of digital EEG, quantitative EEG and brain mapping: report of the American Clinical Neurophysiology Society. Neurology 49, 277–292.
Olichney, J.M., Iragui, V.J., Kutas, M., Nowacki, R., Morris, S., Jeste, D.V., 1998. Relationship between auditory P300 amplitude and age of onset of schizophrenia in older patients. Psychiatry Res. 79, 241–254.
Onofrj, M., Thomas, A., Iacono, D., Luciano, A.L., Di Iorio, A., 2003. The effects of a cholinesterase inhibitor are prominent in patients with fluctuating cognition: a part 3 study of the main mechanism of cholinesterase inhibitors in dementia. Clin. Neuropharmacol. 26, 239–251.
Pascual-Marqui, R.D., 2007a. Discrete, 3D distributed, linear imaging methods of electric neuronal activity. Part 1: exact, zero error localization. arXiv:0710.3341 [math-ph]. Available at: http://arxiv.org/pdf/0710.3341. [Accessed November 19, 2015].
Pascual-Marqui, R.D., 2007b. Coherence and phase synchronization: generalization to pairs of multivariate time series, and removal of zero-lag contributions. arXiv:0706.1776v3 [stat.ME]. Available at: http://arxiv.org/pdf/0706.1776. [Accessed November 19, 2015].
Pascual-Marqui, R.D., 2007c. Instantaneous and lagged measurements of linear and nonlinear dependence between groups of multivariate time series: frequency decomposition. arXiv:0711.1455 [stat.ME]. Available at: http://arxiv.org/abs/0711.1455. [Accessed November 19, 2015].
Pascual-Marqui, R.D., Biscay, R.J., Bosch-Bayard, J., Lehmann, D., Kochi, K., Kinoshita, T., Yamada, N., Sadato, N., 2014. Assessing direct paths of intracortical causal information flow of oscillatory activity with the isolated effective coherence (iCoh). Front. Hum. Neurosci. 8, 448.
Pascual-Marqui, R.D., Lehmann, D., Koukkou, M., Kochi, K., Anderer, P., Saletu, B., Tanaka, H., Hirata, K., John, E.R., Prichep, L., Biscay-Lirio, R., Kinoshita, T., 2011. Assessing interactions in the brain with exact low-resolution electromagnetic tomography. Philos. Trans. A. Math. Phys. Eng. Sci. 369, 3768–3784.
Passero, S., Rocchi, R., Vatti, G., Burgalassi, L., Battistini, N., 1995. Quantitative EEG mapping, regional cerebral blood flow, and neuropsychological function in Alzheimer's disease. Dementia 6, 148–156.
Peavy, G.M., Edland, S.D., Toole, B.M., Hansen, L.A., Galasko, D.R., Mayo, A.M., 2016. Phenotypic differences based on staging of Alzheimer's neuropathology in autopsy-confirmed dementia with Lewy bodies. Parkinsonism Relat. Disord. 31, 72–78.
Pievani, M., de Haan, W., Wu, T., Seeley, W.W., Frisoni, G.B., 2011. Functional network disruption in the degenerative dementias. Lancet Neurol. 10, 829–843.
Pogarell, O., Teipel, S.J., Juckel, G., Gootjes, L., Moller, T., Burger, K., Leinsinger, G., Möller, H.J., Hegerl, U., Hampel, H., 2005. EEG coherence reflects regional corpus callosum area in Alzheimer's disease. J. Neurol. Neurosurg. Psychiatry 76, 109–111.
Pollok, B., Kamp, D., Butz, M., Wojtecki, L., Timmermann, L., Südmeyer, M., Krause, V., Schnitzler, A., 2013. Increased SMA-M1 coherence in Parkinson's disease - Pathophysiology or compensation? Exp. Neurol. 247, 178–181.
Ponomareva, N.V., Selesneva, N.D., Jarikov, G.A., 2003. EEG alterations in subjects at high familial risk for Alzheimer's disease. Neuropsychobiology 48, 152–159.
Pugnetti, L., Baglio, F., Farina, E., Alberoni, M., Calabrese, E., Gambini, A., Di Bella, E., Garegnani, M., Deleonardis, L., Nemni, R., 2010. EEG evidence of posterior cortical disconnection in PD and related dementias. Int. J. Neurosci. 120, 88–98.
Reeves, R.R., Struve, F.A., Patrick, G., 2002. The effects of donepezil on quantitative EEG in patients with Alzheimer's disease. Clin. Electroencephalogr. 33, 93–96.
Reuter-Lorenz, P.A., Mikels, J.A., 2005. A split-brain model of Alzheimer's disease? Behavioral evidence for comparable intra and interhemispheric decline. Neuropsychologia 43, 1307–1317.
Rodriguez, G., Copello, F., Nobili, F., Vitali, P., Perego, G., Nobili, F., 1999. EEG spectral profile to stage Alzheimer's disease. Clin. Neurophysiol. 110, 1831–1837.
Rodriguez, G., Vitali, P., De Leo, C., De Carli, F., Girtler, N., Nobili, F., 2002. Quantitative EEG changes in Alzheimer patients during long-term donepezil therapy. Neuropsychobiology 46, 49–56.
Roks, G., Korf, E.S., van der Flier, W.M., Scheltens, P., Stam, C.J., 2008. The use of EEG in the diagnosis of dementia with Lewy bodies. J. Neurol. Neurosurg. Psychiatry 79, 377–380.
Roman, G.C., Tatemichi, T.K., Erkinjuntti, T., Cummings, J.L., Masdeu, J.C., Garcia, J.H., Amaducci, L., Orgogozo, J.M., Brun, A., Hofman, A., et al., 1993. Vascular dementia: diagnostic criteria for research studies. Report of the NINDS-AIREN International Workshop. Neurology 43, 250–260.
Rosen, W.G., Terry, R.D., Fuld, P.A., Katzman, R., Peck, A., 1980. Pathological verification of ischemic score in differentiation of dementias. Ann. Neurol. 7, 486–488.
Roy, R., Niccolini, F., Pagano, G., Politis, M., 2016. Cholinergic imaging in dementia spectrum disorders. Eur. J. Nucl. Med. Mol. Imaging 43, 1376–1386.
Sankari, Z., Adeli, H., Adeli, A., 2011. Intrahemispheric, interhemispheric, and distal EEG coherence in Alzheimer's disease. Clin. Neurophysiol. 122, 897–906.
Sarro, L., Senjem, M.L., Lundt, E.S., Przybelski, S.A., Lesnick, T.G., Graff-Radford, J., Boeve, B.F., Lowe, V.J., Ferman, T.J., Knopman, D.S., Comi, G., Filippi, M., Petersen, R.C., Jack Jr., C.R., Kantarci, K., 2016. Amyloid-β deposition and regional grey matter atrophy rates in dementia with Lewy bodies. Brain 139 (Pt 10), 2740–2750.
Serizawa, K., Kamei, S., Morita, A., Hara, M., Mizutani, T., Yoshihashi, H., Yamaguchi, M., Takeshita, J., Hirayanagi, K., 2008. Comparison of quantitative EEGs between Parkinson disease and age-adjusted normal controls. J. Clin. Neurophysiol. 25, 361–366.
Silberstein, P., Pogosyan, A., Kühn, A.A., Hotton, G., Tisch, S., Kupsch, A., Dowsey-Limousin, P., Hariz, M.I., Brown, P., 2005. Cortico-cortical coupling in Parkinson's disease and its modulation by therapy. Brain 128 (Pt 6), 1277–1291.
Sloan, E.P., Fenton, G.W., Kennedy, N.S., MacLennan, J.M., 1994. Neurophysiology and SPECT cerebral blood flow patterns in dementia. Electroencephalogr. Clin. Neurophysiol. 91, 163–170.
Snaedal, J., Johannesson, G.H., Gudmundsson, T.E., Blin, N.P., Emilsdottir, A.L., Einarsson, B., Johnsen, K., 2012. Diagnostic accuracy of statistical pattern recognition of electroencephalogram registration in evaluation of cognitive impairment and dementia. Dement. Geriatr. Cogn. Disord. 34, 51–60.

Snaedal, J., Johannesson, G.H., Gudmundsson, T.E., Gudmundsson, S., Pajdak, T.H., Johnsen, K., 2010. The use of EEG in Alzheimer's disease, with and without scopolamine - a pilot study. Clin. Neurophysiol. 121, 836–841.

Soikkeli, R., Partanen, J., Soininen, H., Pääkkönen, A., Riekkinen Sr., P., 1991. Slowing of EEG in Parkinson's disease. Electroencephalogr. Clin. Neurophysiol. 79, 159–165.

Stam, C.J., Jones, B.F., Manshanden, I., van Cappellen van Walsum, A.M., Montez, T., Verbunt, J.P., de Munck, J.C., van Dijk, B.W., Berendse, H.W., Scheltens, P., 2006. Magnetoencephalographic evaluation of resting-state functional connectivity in Alzheimer's disease. Neuroimage 32, 1335–1344.

Stam, C.J., Jones, B.F., Nolte, G., Breakspear, M., Scheltens, P., 2007. Small-world networks and functional connectivity in Alzheimer's disease. Cereb. Cortex 17, 92–99.

Stern, Y., 2017. An approach to studying the neural correlates of reserve. Brain Imaging Behav. 11, 410–416.

Taylor, H., Schmiedt, J.T., Carcak, N., Onat, F., Di Giovanni, G., Lambert, R., Leresche, N., Crunelli, V., David, F., 2014. Investigating local and long-range neuronal network dynamics by simultaneous optogenetics, reverse microdialysis and silicon probe recordings in vivo. J. Neurosci. Methods 235, 83–91.

Teipel, S., Grothe, M.J., Zhou, J., Sepulcre, J., Dyrba, M., Sorg, C., Babiloni, C., 2016. Measuring cortical connectivity in Alzheimer's disease as a brain neural network pathology: toward clinical applications. J. Int. Neuropsychol. Soc. 22, 138–163.

Teramoto, H., Morita, A., Ninomiya, S., Akimoto, T., Shiota, H., Kamei, S., 2016. Relation between resting state front-parietal EEG coherence and executive function in Parkinson's disease. Biomed. Res. Int. 2016, 2845754.

Valladares-Neto, D.C., Buchsbaum, M.S., Evans, W.J., Nguyen, D., Nguyen, P., Siegel, B.V., Stanley, J., Starr, A., Guich, S., Rice, D., 1995. EEG delta, positron emission tomography, and memory deficit in Alzheimer's disease. Neuropsychobiology 31, 173–181.

van Dellen, E., de Waal, H., van der Flier, W.M., Lemstra, A.W., Slooter, A.J., Smits, L.L., van Straaten, E.C., Stam, C.J., Scheltens, P., 2015. Loss of EEG network efficiency is related to cognitive impairment in dementia with Lewy bodies. Mov. Disord. 30, 1785–1793.

van Steenoven, I., Aarsland, D., Weintraub, D., Londos, E., Blanc, F., van der Flier, W.M., Teunissen, C.E., Mollenhauer, B., Fladby, T., Kramberger, M.G., Bonanni, L., Lemstra, A.W., 2016. European DLB Consortium, Cerebrospinal fluid Alzheimer's disease biomarkers across the spectrum of lewy body diseases: results from a large multicenter cohort. J. Alzheimers Dis. 54, 287–295.

Walker, M.P., Ayre, G.A., Cummings, J.L., Wesnes, K., McKeith, I.G., O'Brien, J.T., Ballard, C.G., 2000a. The clinician assessment of fluctuation and the one day fluctuation assessment scale. Two methods assess fluctuating confusion in dementia. Br. J. Psychiatry 177, 252–256.

Walker, M.P., Ayre, G.A., Cummings, J.L., Wesnes, K., Mc Keith, I.G., O'Brien, J.T., Ballard, C.G., 2000b. Quantifying fluctuation in dementia with Lewy bodies, Alzheimer's disease, and vascular dementia. Neurology 54, 1616–1625.

Walker, Z., Possin, K.L., Boeve, B.F., Aarsland, D., 2015. Lewy body dementias. Lancet 386, 1683–1697. Review.

Wolters, E.C., 2001. Intrinsic and extrinsic psychosis in Parkinson's disease. J. Neurol. 248 (Suppl. 3). Review.

Yesavage, J.A., Brink, T.L., Rose, T.L., Lum, O., Huang, V., Adey, M., Leirer, V.O., 1983. Development and validation of a geriatric depression screening scale: a preliminary report. J. Psychiatr. Res. 17, 37–49.

Zhu, L., Ploessl, K., Kung, H.F., 2014. PET/SPECT imaging agents for neurodegenerative diseases. Chem. Soc. Rev. 43, 6683–6691.